

**EXPERIMENTAL SITE WIND AVAILABILITY
STUDY FOR
SAN PO KONG, HONG KONG**

**INVESTIGATION REPORT WWTF012-2009
August 2009**

**Submitted to
Department of Architecture,
The Chinese University of Hong Kong**

EXECUTIVE SUMMARY

At the request of the Department of Architecture, The Chinese University of Hong Kong, on behalf of Planning Department of The Government of Hong Kong Special Administrative Region, a study of wind availability and characteristics for a nominated Study Area in San Po Kong was conducted by the CLP Power Wind/Wave Tunnel Facility (WWTF) at The Hong Kong University of Science and Technology, as part of the “Urban Climate Map and Standards for Wind Environment – Feasibility Study”. The study was undertaken in accordance with the requirements stipulated in the Australasian Wind Engineering Society Quality Assurance Manual, AWES-QAM-1-2001 (2001) and the American Society of Civil Engineers Manual and Report on Engineering Practice No. 67 for Wind Tunnel Studies of Buildings and Structures (1999). The study was also conducted in accordance with the recommendations of Planning Department’s Feasibility Study for Establishment of Air Ventilation Assessment System – Final Report (2005) and Technical Guide for Air Ventilation Assessment for Developments in Hong Kong (2006).

A 1:2000 scale topography study was undertaken to determine the effects of local topography and the surrounding urban environment on mean wind direction, mean wind speed and turbulence intensity at a nominated Study Area in San Po Kong.

A miniature dynamic pressure (Cobra) probe was used to take measurements of the longitudinal, lateral and vertical components of wind speed, at 22.5° increments for the full 360° azimuth, i.e. for sixteen (16) wind directions, and at nine (9) elevations to determine profiles of mean wind speed and turbulence intensity above the Study Area. The results will be used as input boundary conditions for subsequent detailed benchmarking studies. The 1:2000 scale topographical model included the surrounding area up to a distance of up to approximately 10 km from the Study Area.

The topography study results were combined with WWTF’s statistical model of the Hong Kong non-typhoon wind climate, based on measurements of non-typhoon winds taken by Hong Kong Observatory at Waglan Island during the period of 1953 – 2006 inclusive, to determine wind roses corresponding to annual and summer mean wind speeds at the Study Area.

In general, the annual prevailing wind characteristics corresponding to non-typhoon winds at an elevation of 500 mPD above the San Po Kong Study Area were similar to the overall characteristics of non-typhoon winds approaching the Hong Kong region, although the magnitudes of the directional wind speeds were reduced. More significant changes were observed in the summer prevailing wind characteristics, which is mainly due to the effects of hilly terrain on Hong Kong Island to the south-west of the Study Area.

Significant reductions in the measured magnitudes of wind speed were mainly caused by the mountains located to the north-west of the Study Area, such as Lion Rock, north-east of the Study Area, such as Tate's Cairn, and east of the Study Area on Kowloon, and on Hong Kong Island. Those mountains significantly affected the directional characteristics for wind directions of 67.5°, 90°, 225° and 315°. Winds approaching the Study Area from 157.5° were the least affected due to the relatively open sea exposure at the Lei Yue Mun entrance to Victoria Harbour.

TABLE OF CONTENTS

1	INTRODUCTION	1
2	ANALYSIS OF THE HONG KONG WIND CLIMATE	2
3	WIND TUNNEL STUDY	5
3.1	Modelling the Natural Wind	5
3.2	Physical Model of the Study Area	8
3.3	Experimental and Analysis Procedures	9
4	EXPERIMENTAL RESULTS AND DISCUSSION	10
4.1	Wind characteristics of the San Po Kong Study Area	11
5	CONCLUSIONS	15
6	REFERENCES	17
	APPENDIX A TABULATED RESULTS FOR SAN PO KONG	51
	APPENDIX B AXIS SYSTEM OF THE COBRA PROBE	59

LIST OF FIGURES

Figure 1:	San Po Kong Study Area	21
Figure 2:	Location of the San Po Kong Study Area	22
Figure 3:	Wind rose for annual non-typhoon winds, Waglan Island, corrected to 500 mPD above open water, 1953-2006	23
Figure 4:	Wind rose for summer non-typhoon winds, Waglan Island corrected to 500 mPD above open water, 1953-2006	24
Figure 5:	Wind tunnel test sections at the CLP Power Wind/Wave Tunnel Facility	25
Figure 6:	Simulated mean wind speed and turbulence intensity profiles of approach wind	26
Figure 7:	Longitudinal turbulence spectrum of approach wind	26
Figure 8:	1:2000 scale topographical model of San Po Kong in low speed test section of the CLP Power Wind/Wave Tunnel Facility	27-28
Figure 9a:	Wind characteristics for San Po Kong, 22.5°	29
Figure 9b:	Mean wind directions for San Po Kong, 22.5°	29
Figure 10a:	Wind characteristics for San Po Kong, 45°	30
Figure 10b:	Mean wind directions for San Po Kong, 45°	30
Figure 11a:	Wind characteristics for San Po Kong, 67.5°	31
Figure 11b:	Mean wind directions for San Po Kong, 67.5°	31
Figure 12a:	Wind characteristics for San Po Kong, 90°	32
Figure 12b:	Mean wind directions for San Po Kong, 90°	32
Figure 13a:	Wind characteristics for San Po Kong, 112.5°	33
Figure 13b:	Mean wind directions for San Po Kong, 112.5°	33
Figure 14a:	Wind characteristics for San Po Kong, 135°	34
Figure 14b:	Mean wind directions for San Po Kong, 135°	34
Figure 15a:	Wind characteristics for San Po Kong, 157.5°	35
Figure 15b:	Mean wind directions for San Po Kong, 157.5°	35
Figure 16a:	Wind characteristics for San Po Kong, 180°	36
Figure 16b:	Mean wind directions for San Po Kong, 180°	36

Figure 17a:	Wind characteristics for San Po Kong, 202.5°	37
Figure 17b:	Mean wind directions for San Po Kong, 202.5°	37
Figure 18a:	Wind characteristics for San Po Kong, 225°	38
Figure 18b:	Mean wind directions for San Po Kong, 225°	38
Figure 19a:	Wind characteristics for San Po Kong, 247.5°	39
Figure 19b:	Mean wind directions for San Po Kong, 247.5°	39
Figure 20a:	Wind characteristics for San Po Kong, 270°	40
Figure 20b:	Mean wind directions for San Po Kong, 270°	40
Figure 21a:	Wind characteristics for San Po Kong, 292.5°	41
Figure 21b:	Mean wind directions for San Po Kong, 292.5°	41
Figure 22a:	Wind characteristics for San Po Kong, 315°	42
Figure 22b:	Mean wind directions for San Po Kong, 315°	42
Figure 23a:	Wind characteristics for San Po Kong, 337.5°	43
Figure 23b:	Mean wind directions for San Po Kong, 337.5°	43
Figure 24a:	Wind characteristics for San Po Kong, 360°	44
Figure 24b:	Mean wind directions for San Po Kong, 360°	44
Figure 25:	Wind rose for annual, non-typhoon winds for San Po Kong, corrected to 50 mPD	45
Figure 26:	Wind rose for annual, non-typhoon winds for San Po Kong, corrected to 100 mPD	46
Figure 27:	Wind rose for annual, non-typhoon winds for San Po Kong, corrected to 200 mPD	47
Figure 28:	Wind rose for annual, non-typhoon winds for San Po Kong, corrected to 500 mPD	48
Figure 29:	Wind rose for summer, non-typhoon winds for San Po Kong, corrected to 50 mPD	49
Figure 30:	Wind rose for summer, non-typhoon winds for San Po Kong, corrected to 100 mPD	50
Figure 31:	Wind rose for summer, non-typhoon winds for San Po Kong, corrected to 200 mPD	51
Figure 32:	Wind rose for summer, non-typhoon winds for San Po Kong, corrected to 500 mPD	52

LIST OF TABLES

Table A1: Site wind characteristics of San Po Kong at 22.5°	51
Table A2: Site wind characteristics of San Po Kong at 45°	51
Table A3: Site wind characteristics of San Po Kong at 67.5°	51
Table A4: Site wind characteristics of San Po Kong at 90°	52
Table A5: Site wind characteristics of San Po Kong at 112.5°	52
Table A6: Site wind characteristics of San Po Kong at 135°	52
Table A7: Site wind characteristics of San Po Kong at 157.5°	52
Table A8: Site wind characteristics of San Po Kong at 180°	53
Table A9: Site wind characteristics of San Po Kong at 202.5°	53
Table A10: Site wind characteristics of San Po Kong at 225°	53
Table A11: Site wind characteristics of San Po Kong at 247.5°	53
Table A12: Site wind characteristics of San Po Kong at 270°	54
Table A13: Site wind characteristics of San Po Kong at 292.5°	54
Table A14: Site wind characteristics of San Po Kong at 315°	54
Table A15: Site wind characteristics of San Po Kong at 337.5°	54
Table A16: Site wind characteristics of San Po Kong at 360°	55
Table A17: Percentage occurrence for annual, non-typhoon directional winds at 50 mPD	55
Table A18: Percentage occurrence for annual, non-typhoon directional winds at 100 mPD	55
Table A19: Percentage occurrence for annual, non-typhoon directional winds at 200 mPD	56
Table A20: Percentage occurrence for annual, non-typhoon directional winds at 500 mPD	56
Table A21: Percentage occurrence for summer, non-typhoon directional winds at 50 mPD	57
Table A22: Percentage occurrence for summer, non-typhoon directional winds at 100 mPD	57
Table A23: Percentage occurrence for summer, non-typhoon directional winds at 200 mPD	58
Table A24: Percentage occurrence for summer, non-typhoon directional winds at 500 mPD	58

1 INTRODUCTION

At the request of the Department of Architecture, The Chinese University of Hong Kong, on behalf of Planning Department of The Government of Hong Kong Special Administrative Region, a study of wind availability and characteristics was conducted by the CLP Power Wind/Wave Tunnel Facility (WWTF) at The Hong Kong University of Science and Technology for a nominated Study Area in San Po Kong, as part of the “Urban Climate Map and Standards for Wind Environment – Feasibility Study”. The study was undertaken in accordance with the requirements stipulated in the Australasian Wind Engineering Society Quality Assurance Manual, AWES-QAM-1-2001 (2001) and the American Society of Civil Engineers Manual and Report on Engineering Practice No. 67 for Wind Tunnel Studies of Buildings and Structures (1999). The study was also conducted in accordance with the recommendations of Planning Department’s Feasibility Study for Establishment of Air Ventilation Assessment System – Final Report (2005) and Technical Guide for Air Ventilation Assessment for Developments in Hong Kong (2006).

The Study Area of San Po Kong, centred close to the junction of Tseuk Luk Street and Tai Yau Street, has a diameter of approximately 1000 m, as shown in Figures 1 and 2. A 1:2000 scale topography study was undertaken to determine the effects of local topography and the surrounding urban environment on mean wind speeds and turbulence intensities at the Study Area. The topography study results were combined with WWTF’s statistical model of the Hong Kong non-typhoon wind climate, based on measurements of non-typhoon winds taken by Hong Kong Observatory at Waglan Island during the period of 1953 – 2006 inclusive, to determine site-specific annual and summer wind roses for hourly mean wind speeds.

2 ANALYSIS OF THE HONG KONG WIND CLIMATE

Waglan Island, located approximately 5 km southeast of Hong Kong Island, has been used by Hong Kong Observatory (HKO), formerly The Royal Observatory, Hong Kong, for the collection of long-term wind data since December 1952. Due to its location, relative lack of development over the past 50 years and its generally uninterrupted exposure to winds, data collected at Waglan Island is considered to be of the highest quality available for wind engineering purposes in Hong Kong and representative of winds approaching the Hong Kong region. Wind speed and direction measurements at Waglan Island are essentially free from the interference effects of nearby developments and they can be position corrected to account for the effects of the location and height of the anemometer stations and the effects of the surrounding topography and buildings.

Waglan Island wind records have been analysed previously in studies of the Hong Kong wind climate, most notably by Davenport et al. (1984), Melbourne (1984) and Hitchcock et al. (2003). Melbourne (1984) conducted wind tunnel model studies to determine directional factors relating wind speeds at each anemometer location to the wind speed at an elevation equivalent to 50 mPD in the free stream flow and concluded that:

- Measurements taken during the period 1 January 1964 to 11 July 1966 inclusive were directly and adversely affected by the effects of the building on which it was mounted; therefore, records from that period were excluded from that study.

- The anemometer correction factors for mean wind speeds show some sensitivity to the modelled approach flow but they are not strongly dependent on the modelled approach profiles.
- The largest magnitude speed-up effects occur for winds approaching from approximately 67.5°, 180°, 270° and 360°.
- The largest magnitude slow-down effects occur for winds approaching from approximately 112.5°, 225° and 315°.

In the study conducted by Hitchcock et al. (2003), wind tunnel tests were undertaken to correct wind records for position and topographical effects at the four anemometer locations used since 1952, with the exception of the location used during the period 1 January 1964 to 11 July 1966 inclusive. In that study, thermal (hotwire) anemometer measurements were taken at 22.5° intervals for the full 360° azimuth relating wind speeds at anemometer height to wind speeds at an elevation equivalent to 200 mPD in the free stream. The directional characteristics of the former anemometer sites were found to be similar to those discussed by Davenport et al. (1984) and Melbourne (1984), whereas the current anemometer site is much less affected than its predecessors, due mainly to its additional height.

Correction factors were determined and subsequently applied to non-typhoon wind data collected at Waglan Island to determine a probability distribution of directional mean wind speeds for Hong Kong. The corresponding annual wind rose for mean wind speeds at an elevation equivalent to 500 mPD above open water is presented in Figure 3 and indicates that, on an annual basis, prevailing and strong non-typhoon winds approaching Hong Kong occur mainly from the north-east quadrant and, to a

lesser extent, the south-west. The summer (i.e. June, July, August) wind rose for mean wind speeds at an elevation equivalent to 500 mPD above open water is presented in Figure 4. In contrast to the corresponding annual wind rose, prevailing and strong non-typhoon winds approaching Hong Kong during summer months occur mainly from the south-east and south-west quadrants.

In Figures 3 and 4, mean wind speeds are segregated into four categories (0 – 3.3 m/s, 3.4 – 7.9 m/s, 8.0 – 13.8 m/s and greater than 13.8 m/s) that are indicated by the thickness of the bars for the 16 cardinal wind directions. The length of the bars indicates the average percentage of occurrence per year. For example, Figure 3 illustrates that, on an annual basis, east winds occur approximately 24% of the time and hourly mean wind speeds exceed 13.8 m/s approximately 6% of the time at an elevation of 500 mPD.

3 WIND TUNNEL STUDY

The wind tunnel test techniques used in this investigation are in accordance with the procedures and recommendations of the Australasian Wind Engineering Society Quality Assurance Manual, AWES QAM-1-2001 (2001) and the American Society of Civil Engineers Manual and Report on Engineering Practice No. 67 for Wind Tunnel Studies of Buildings and Structures (1999). Those requirements cover the satisfactory modelling of the turbulent natural wind, the accuracy of the wind tunnel models, experimental and analysis procedures, and quality assurance.

3.1 Modelling the Natural Wind

Air moving relative to the Earth's surface has frictional forces imparted on it, which effectively cause it to be slowed down. These forces have a decreasing effect on airflow as the height above ground increases, generally resulting in mean wind speed increasing with height to a point where the effects of surface drag become negligible. In wind engineering, a convenient measure of the thickness of the atmospheric boundary layer is commonly referred to as the gradient height which will vary depending on the surrounding surface roughness over which the air will flow. Obstacles to air flow can vary from relatively large expanses of smooth, open water, to vegetation such as forests, built-up environments such as city centres, and large, rugged mountain ranges. The resulting gradient heights typically vary from several hundred metres to in excess of 1000 m.

Winds within the atmospheric boundary layer are also usually highly turbulent or gusty. Turbulence intensity is a measure of the gustiness of wind due to eddies and

vortices generated by frictional effects at surface level, the roughness of the terrain over which air is flowing and convective effects due to opposing movements of air masses of different temperature. In typical atmospheric boundary layer flow, turbulence intensity generally decreases with height. Closer to the ground, at pedestrian level for example, the magnitude of the turbulence intensity can be very large due to the effects of wind flowing around buildings and other structures.

In conducting wind tunnel model studies of wind characteristics and wind effects on and around tall buildings and other structures on the surface of the Earth, it is necessary to adequately simulate the relevant characteristics of atmospheric boundary layer flow. WWTF's boundary layer wind tunnel test sections can be used to simulate atmospheric boundary layer flow over various types of terrain, ranging from open terrain, such as open water, to urban or mountainous terrain.

WWTF comprises two long fetch boundary layer wind tunnel test sections as shown in Figure 5. The 28 m long high speed test section has a 3 m wide \times 2 m high working section and a maximum free stream wind speed of approximately 30 m/s. The 40 m long low speed test section has a 5 m wide \times 4 m high working section and a maximum free-stream wind speed of approximately 10 m/s. Various terrains can be modelled in either test section at length scales ranging from approximately 1:5000 to 1:50.

The characteristics of the wind flow in the low speed test section can be modified through the use of devices such as spires, grids, and fences to model various atmospheric boundary layer flows. For the current study, WWTF's low speed test section was calibrated by using various roughness elements to simulate the wind

speed and turbulence intensity characteristics corresponding to wind flow above open water. The mean wind speed profile of the wind flow approaching the Study Area was simulated in accordance with the power law expression, defined in Equation (1), specified in Planning Department's Feasibility Study for Establishment of Air Ventilation Assessment System – Final Report (2005).

$$\frac{V_{z,\text{open}}}{V_{\text{ref,open}}} = \left(\frac{z}{z_{\text{ref}}} \right)^\alpha \quad (1)$$

where

$V_{z,\text{open}}$ = mean wind speed at a height z above open water terrain (m/s);

$V_{\text{ref,open}}$ = mean wind speed at a height z_{ref} above open water terrain (m/s);

z = height above zero plane displacement height (m);

z_{ref} = a suitable reference height above open water terrain (m);

α = a power law exponent, which is a constant commensurate with the terrain roughness, taken as 0.15 for this study.

The turbulence intensity profile of the approaching wind flow was simulated in accordance with Terrain category 2 stipulated in Australian/New Zealand Standard AS/NZS 1170.2:2002, i.e. corresponding to non-typhoon wind flow above rough open water surfaces.

The simulated mean wind speed and turbulence intensity profiles were generally within $\pm 10\%$ of the target mean speed and turbulence intensity profiles and they are presented in Figure 6. The spectrum of longitudinal turbulence of the approaching

wind flow measured at an elevation equivalent to 500 mPD in prototype scale is presented in Figure 7.

3.2 Physical Model of the Study Area

WWTF has a 1:2000 scale topographical model of the New Territories, Kowloon and Hong Kong Island fabricated at 20 m contour intervals from information acquired from the Survey and Mapping Office of The Government of the Hong Kong Special Administrative Region (HKSAR) Lands Department. The relevant sections of the topographical model were updated to include all known current buildings and the major topographical features in the urban landscapes of Hong Kong Island, Kowloon Peninsula and the New Territories. For all wind directions tested, the wind tunnel model included surrounding areas within a distance of up to approximately 10 km from the Study Area.

The topographical model was updated to include greater detail within a zone from 500 m up to approximately 1000 m from the Study Area. In accordance with information supplied by the Department of Architecture of The Chinese University of Hong Kong during the period between 13 January 2009 to 10 March 2009, all specified committed developments and all known existing buildings and structures at the time of testing were included in the model to represent their effects on wind flow approaching the Study Area. Beyond the 1000 m radius, the topographical model included roughness representative of the surrounding areas. A representative view of the 1:2000 scale topographical model used in the current study is shown in Figure 8.

3.3 Experimental and Analysis Procedures

The terrain surrounding the Study Area comprises complex mixtures of open water, urban and built-up environment, and mountainous areas on Hong Kong Island and Kowloon Peninsula. Winds approaching the modelled region were scaled to simulate non-typhoon winds flowing over open water and the topographical model was used to determine the modifying effects of the surrounding complex terrain on the wind speed and turbulence intensity above the Study Area.

Wind tunnel measurements were taken using a miniature dynamic pressure probe, a Cobra probe manufactured by Turbulent Flow Instrumentation Pty Ltd, at 22.5° intervals for the full 360° azimuth (i.e. 16 wind directions), where a wind direction of 0° or 360° corresponds to an incident wind approaching the Study Area directly from the north, 90° corresponds to an incident wind approaching the Study Area directly from the east, etc. For each wind direction tested, mean wind speeds and turbulence intensities were measured at elevations equivalent to 25, 50, 75, 100, 150, 200, 300, 400 and 500 mPD in prototype scale, above the centre of the Study Area.

While measurements were taken at the Study Area, all buildings within a diameter of 1000 m of the centre of the Study Area were removed from the wind tunnel model for all measured wind directions. All buildings within the diameter of 1000 m will be included in the proximity model for the 1:400 scale detailed benchmarking study to directly account for their effects on the wind flow within the Study Area.

4 EXPERIMENTAL RESULTS AND DISCUSSION

For each wind direction tested, results of the 1:2000 scale topography study are presented in graphical format in Figures 9 to 24 inclusive and in tabular format in Appendix A. In Figures 9a to 24a, the normalised wind characteristics include the measured mean resultant wind speed profiles and turbulence intensity profiles. Mean wind speed profiles were determined by normalising the local mean wind speeds with respect to the mean wind speed of the approaching wind flow measured at an elevation equivalent to 500 mPD, as defined in Equation (2). Vertical profiles of turbulence intensity, defined in Equation (3), are also presented in Figures 9a to 24a. Yaw and pitch angles, i.e. the lateral and vertical deviations, respectively, of the local mean wind direction relative to the approaching mean wind direction, are presented in Figures 9b to 24b inclusive. The sign conventions used to define yaw angles and pitch angles are provided in Appendix B.

$$\text{normalised mean wind speed} = \frac{V_{z,\text{site},i}}{V_{500,\text{open},i}} \quad (2)$$

$$\text{turbulence intensity} = \frac{\sigma_{z,\text{site},i}}{V_{z,\text{site},i}} \quad (3)$$

In Equations (2) and (3), $V_{z,\text{site},i}$ is the resultant mean wind speed above the site centre at an elevation $z = 25, 50, 75, 100, 150, 200, 300, 400$ or 500 mPD in prototype scale) for an approaching wind direction i , where i equals to $22.5^\circ, 45^\circ, 67.5^\circ, 90^\circ, 112.5^\circ, 135^\circ, 157.5^\circ, 180^\circ, 202.5^\circ, 225^\circ, 247.5^\circ, 270^\circ, 292.5^\circ, 315^\circ, 337.5^\circ$ or 360° ; $V_{500,\text{open},i}$ is the resultant mean wind speed of the approaching wind at an elevation equivalent to 500 mPD in prototype scale for an approaching wind direction, i ; and $\sigma_{z,\text{site},i}$ is the

standard deviation of the fluctuating resultant wind speed above the site for an approaching wind direction i . The profiles of resultant mean wind speed and turbulence intensity will be used as input boundary conditions for the detailed benchmarking study for the Study Area.

The topography study measurements were also used to determine directional factors for the 16 measured wind directions, relating the mean wind speeds at elevations equivalent to 50, 100, 200 and 500 mPD above the Study Area to the mean wind speed of the approach flow at a reference height of 500 mPD. Those directional factors were then applied to WWTF's Hong Kong non-typhoon wind climate model, derived from HKO's Waglan Island wind data as discussed in Section 2 of this report, to determine site-specific wind roses pertaining to annual and summer hourly mean wind speeds at elevations of 50, 100, 200 and 500 mPD above the Study Area. The annual wind roses are presented in Figures 25 to 28 inclusive for elevations of 50, 100, 200 and 500 mPD above the San Po Kong Study Area, respectively. The summer wind roses are presented in Figures 29 to 32 inclusive for elevations of 50, 100, 200 and 500 mPD above the San Po Kong Study Area, respectively. Wind rose data are presented in tabular format in Appendix A.

4.1 Wind characteristics of the San Po Kong Study Area

The nominated Study Area in San Po Kong is located approximately 1.8 km to the north of the seafront of Kai Tak airport. It is surrounded by mountains ranging from the north-west to east, as shown in Figures 1 and 2. The major mountains are Lion Rock, approximately 2.6 km to the north-west of the Study Area with an elevation of 490 mPD; Tate's Cairn, approximately 3.5 km to the north-east of the Study Area

with an elevation of 580 mPD; and Kowloon Peak, approximately 2.6 km to the north east to east of the Study Area with an elevation of 600 mPD. Wong Tai Sin, located to the north of the Study Area, and Ngau Chi Wan, located to the east of the Study Area, are occupied by medium-rise public housing. To the south of the Study Area, the former Kai Tak airport is planned for major redevelopment and it will include a mix of residential, commercial and recreational areas. To the west of the Study Area, Kowloon City is occupied predominantly by low-rise and densely distributed buildings, while the Lok Fu area is occupied by medium-rise public housing.

Significant overall reductions to the magnitude of the mean wind speed profiles were measured for wind directions of 22.5°, 45°, 67.5°, 315° and 337.5° for all measured elevations due to the effects of the surrounding mountains. The most significant reduction was measured at a wind direction of 67.5°, with magnitudes of turbulence intensity of around 30%. This is attributed to the flow separation created by the ridge of Kowloon Peak at an elevation of 600 mPD.

For wind directions of 0° (360°), 90° and 112.5°, mean wind speeds measured below an elevation of 200 mPD were reduced significantly, with correspondingly higher magnitudes of turbulence intensity, which is attributed to a combination of the surrounding buildings and mountains. Similar effects were observed at wind directions of 180°, 202.5° and 225°, for which the corresponding mean wind speeds are affected by the buildings in the Kai Tak redevelopment area and the mountains on Hong Kong Island.

For wind directions of 135°, 247.5°, 270° and 292.5°, mean wind speeds measured at elevations below 200 mPD were also reduced significantly, with correspondingly higher magnitudes of turbulence intensity. These characteristics are attributed to the effects of long fetches of more than 4 km of densely distributed buildings upstream of the Study Area. For 247.5°, 270° and 292.5°, this includes areas on the Kowloon Peninsula. For 135°, this includes the region extending from Kwun Tong to Yau Tong.

Winds approaching the Study Area from a direction of 157.5° are the least affected, particularly at higher elevations, due to the fetch of open sea at the Lei Yue Mun entrance to Victoria Harbour. At elevations below 150 mPD, mean wind speeds were reduced due to the effects of the surrounding buildings.

Significant yaw angles, i.e. exceeding $\pm 11.25^\circ$, were measured at elevations below 400 mPD for wind directions of 67.5°, 90°, 225° and 315° due to the effects of the surrounding mountains.

A comparison of the annual and summer wind roses at 500 mPD above open water presented in Figures 3 and 4 to those for the San Po Kong Study Area in Figures 28 and 32 highlights the reductions in the overall magnitudes of wind speed. The yaw angle measured for a wind direction of 225° significantly affects the summer wind characteristics, as shown in Figure 4 and Figure 32. The corresponding changes observed in annual wind rose were less significant, although the effects on south-westerly winds is still readily apparent in Figure 28.

The annual and summer wind roses corresponding to elevations of 50, 100 and 200 mPD above the San Po Kong Study Area in Figures 25, 26, 27, 29, 30 and 31 demonstrates further reductions in the overall magnitudes of wind speed. The yaw angles measured for wind directions of 0° , 67.5° , 90° , 225° and 315° are largely responsible for the significant changes to the directional characteristics of the wind roses at the various elevations presented.

5 CONCLUSIONS

A study of wind availability and characteristics was conducted by the CLP Power Wind/Wave Tunnel Facility at The Hong Kong University of Science and Technology for the nominated Study Area in San Po Kong as part of the “Urban Climate Map and Standards for Wind Environment – Feasibility Study”. The study was conducted at the request of the Department of Architecture, The Chinese University of Hong Kong, on behalf of Planning Department of The Government of Hong Kong Special Administrative Region.

A 1:2000 scale topography study was undertaken to determine the effects of local topography and the surrounding urban environment on mean wind speeds and turbulence intensities above the Study Area. The topography study results were subsequently combined with a statistical model of the Hong Kong wind climate, based on measurements of non-typhoon winds taken by Hong Kong Observatory at Waglan Island, to determine directional wind characteristics and availability for the San Po Kong Study Area.

In general, the annual prevailing wind characteristics corresponding to non-typhoon winds at an elevation of 500 mPD above the San Po Kong Study Area were similar to the overall characteristics of non-typhoon winds approaching the Hong Kong region, although the magnitudes of the directional wind speeds were reduced. More significant changes were observed in the summer prevailing wind characteristics which is mainly due to the effects of hilly terrain on the Hong Kong Island at the south-west of the Study Area.

Significant reductions in the measured magnitudes of wind speed were mainly caused by the mountains located to the north-west of the Study Area, such as Lion Rock, north-east of the Study Area, such as Tate's Cairn, and east of the Study Area on Kowloon, and on Hong Kong Island. Those mountains significantly affected the directional characteristics for wind directions of 67.5°, 90°, 225° and 315°. Winds approaching the Study Area from 157.5° were the least affected due to the relatively open sea exposure at Lei Yue Mun entrance to Victoria Harbour.

6 REFERENCES

Australasian Wind Engineering Society (2001), Wind Engineering Studies of Buildings, AWES-QAM-1-2001.

Buildings Department (HKSAR) (2004), Code of Practice on Wind Effects in Hong Kong.

Davenport, A.G., Georgiou, P.N., Mikić, M., Surry, D. and Kythe, G. (1984), The wind climate of Hong Kong, Proceedings of the Third International Conference on Tall Buildings, Hong Kong and Guangzhou, pp 454 – 460.

Hitchcock, P.A., Kwok, K.C.S. and Yu, C.W. (2003), A study of anemometer measurements at Waglan Island, Hong Kong, Technical Report WWTF002-2003, CLP Power Wind/Wave Tunnel Facility, The Hong Kong University of Science and Technology.

Manual of practice for wind tunnel studies of buildings and structures (1999), Editor Nicholas Isyumov, Task Committee on Wind Tunnel Testing of Buildings and Structures, Aerodynamics Committee, Aerospace Division, American Society of Civil Engineers.

Melbourne, W.H. (1984), Design wind data for Hong Kong and surrounding coastline, Proceedings of the Third International Conference on Tall Buildings, Hong Kong and Guangzhou, pp 461 – 467.

Planning Department, The Government of the Hong Kong Special Administrative Region (2005), Feasibility Study for Establishment of Air Ventilation Assessment – Final Report, Department of Architecture, The Chinese University of Hong Kong.

Planning Department, The Government of the Hong Kong Special Administrative Region (2006), Technical Guide for Air Ventilation Assessment for Developments in Hong Kong.

Planning Department, The Government of the Hong Kong Special Administrative Region (2006), Urban Climatic Map and Standards for Wind Environment-Feasibility Study (Inception Report), The Chinese University of Hong Kong.

Planning Department, The Government of the Hong Kong Special Administrative Region (2006), Urban Climatic Map and Standards for Wind Environment-Feasibility Study (Working Paper 2A: Methodologies of Area Selection for Benchmarking), The Chinese University of Hong Kong.

Standards Australia/Standards New Zealand (2002), Australia/New Zealand Standard Structural design actions Part 2: Wind actions, AS/NZS 1170.2:2002.



Figure 1: San Po Kong Study Area



Figure 2: Location of the San Po Kong Study Area

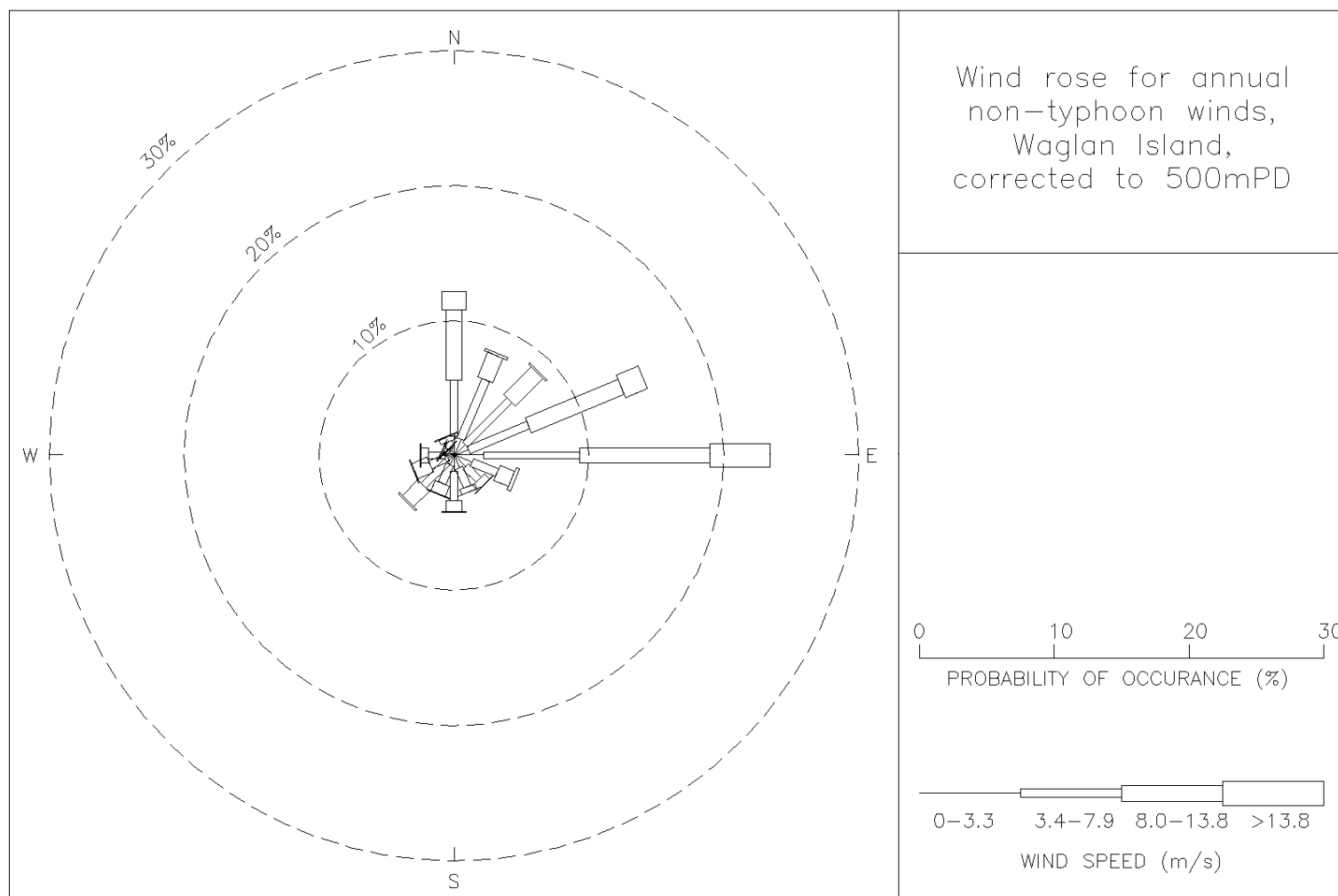


Figure 3: Wind rose for annual non-typhoon winds, Waglan Island, corrected to 500 mPD above open water, 1953-2006

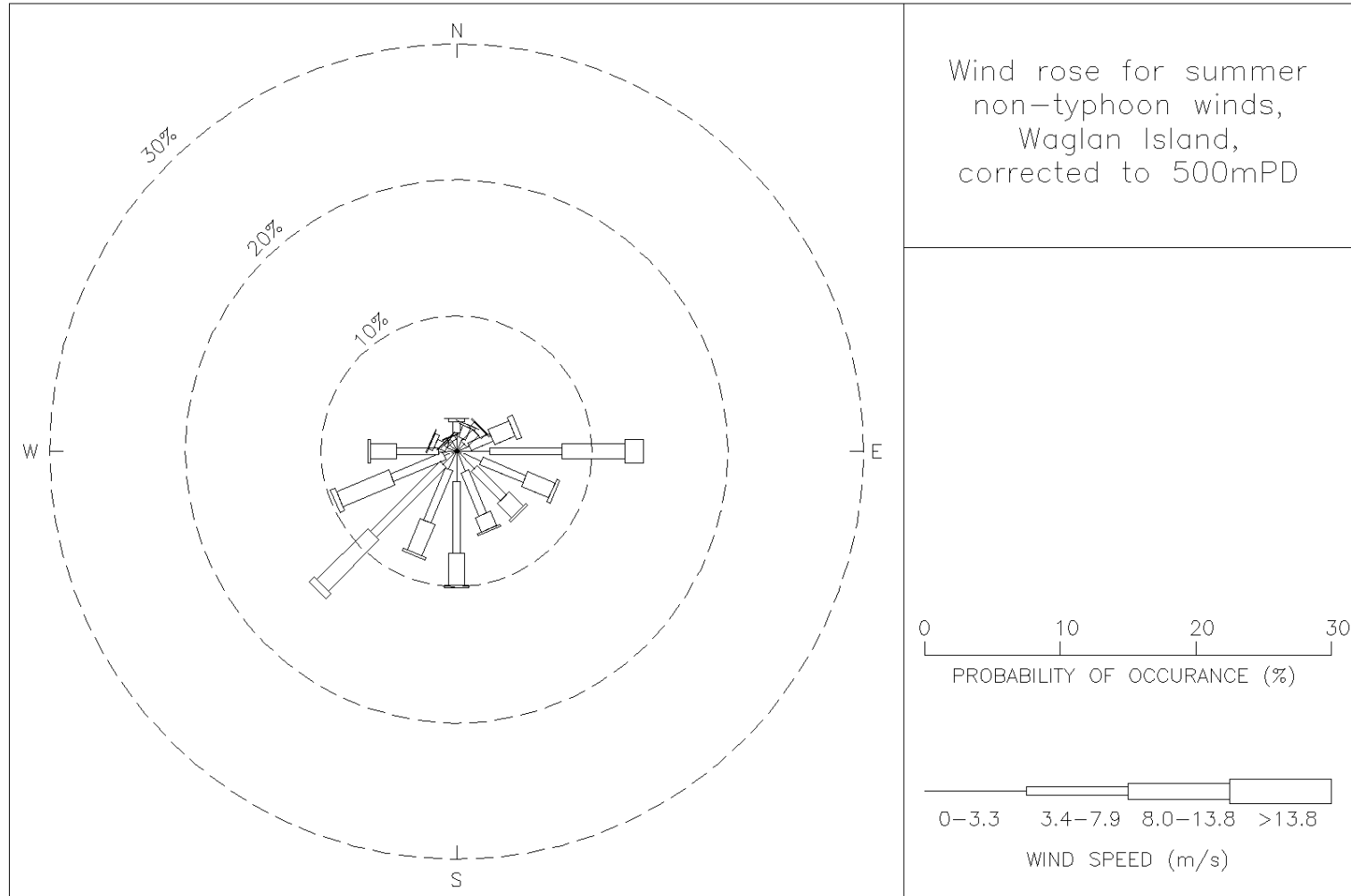


Figure 4: Wind rose for summer non-typhoon winds, Waglan Island corrected to 500 mPD above open water, 1953-2006

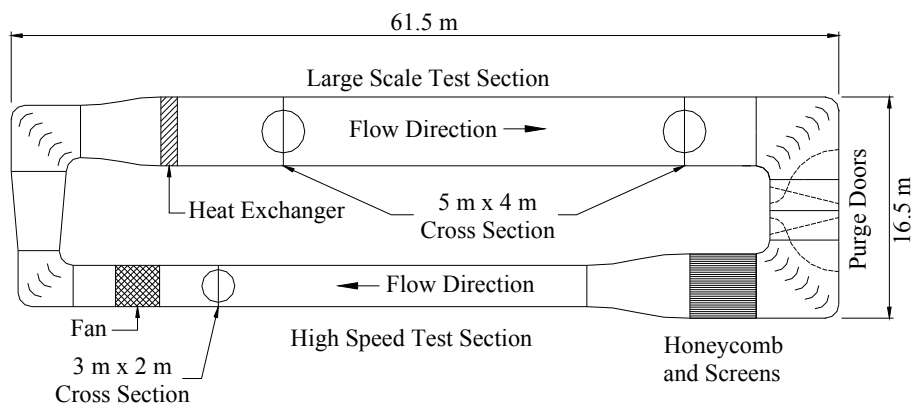


Figure 5: Wind tunnel test sections at the CLP Power Wind/Wave Tunnel Facility

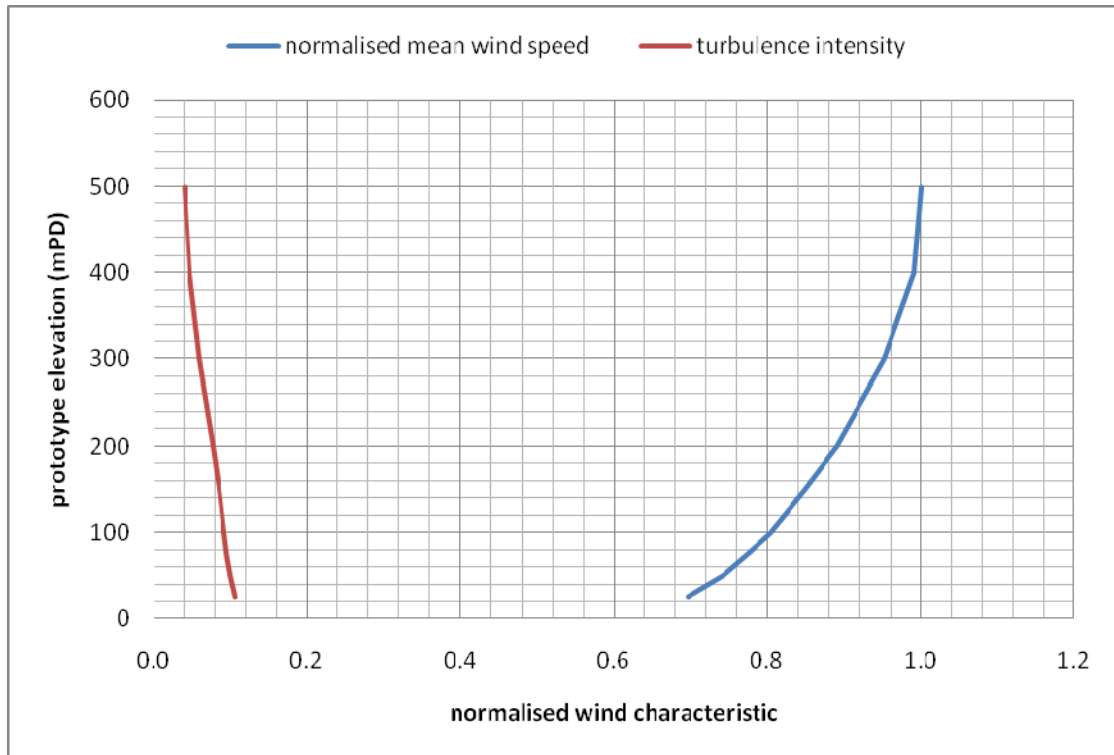


Figure 6: Simulated mean wind speed and turbulence intensity profiles of approach wind

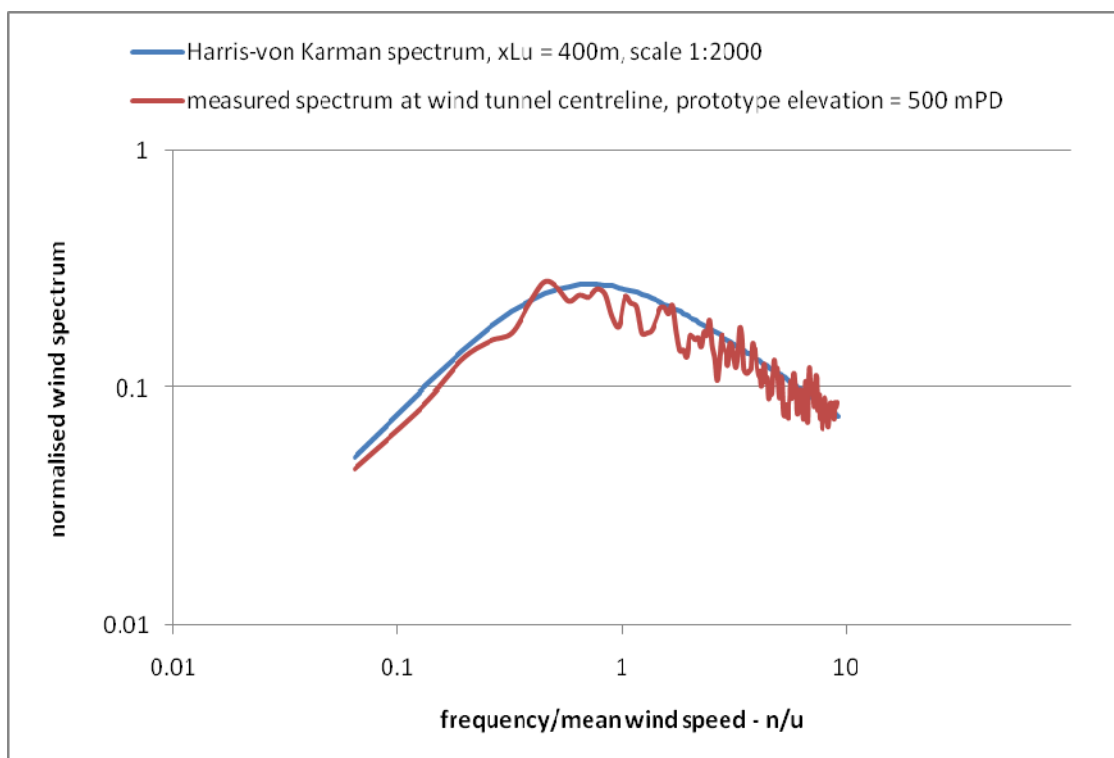


Figure 7: Longitudinal turbulence spectrum of approach wind



(a) North wind direction, 360°



(b) East wind direction, 90°



(c) South wind direction, 180°



(d) West wind direction, 270°

Figure 8: 1:2000 scale topographical model of San Po Kong in the low speed test section of the CLP Power Wind/Wave Tunnel Facility

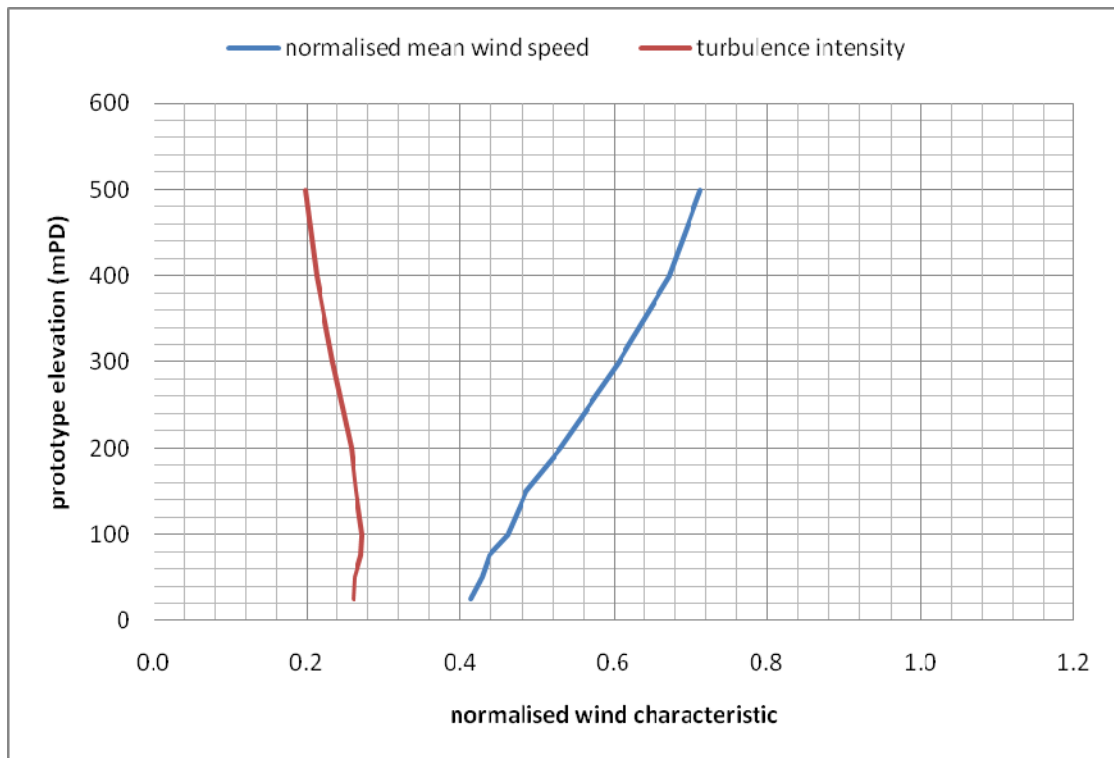


Figure 9a: Wind characteristics for San Po Kong, 22.5°

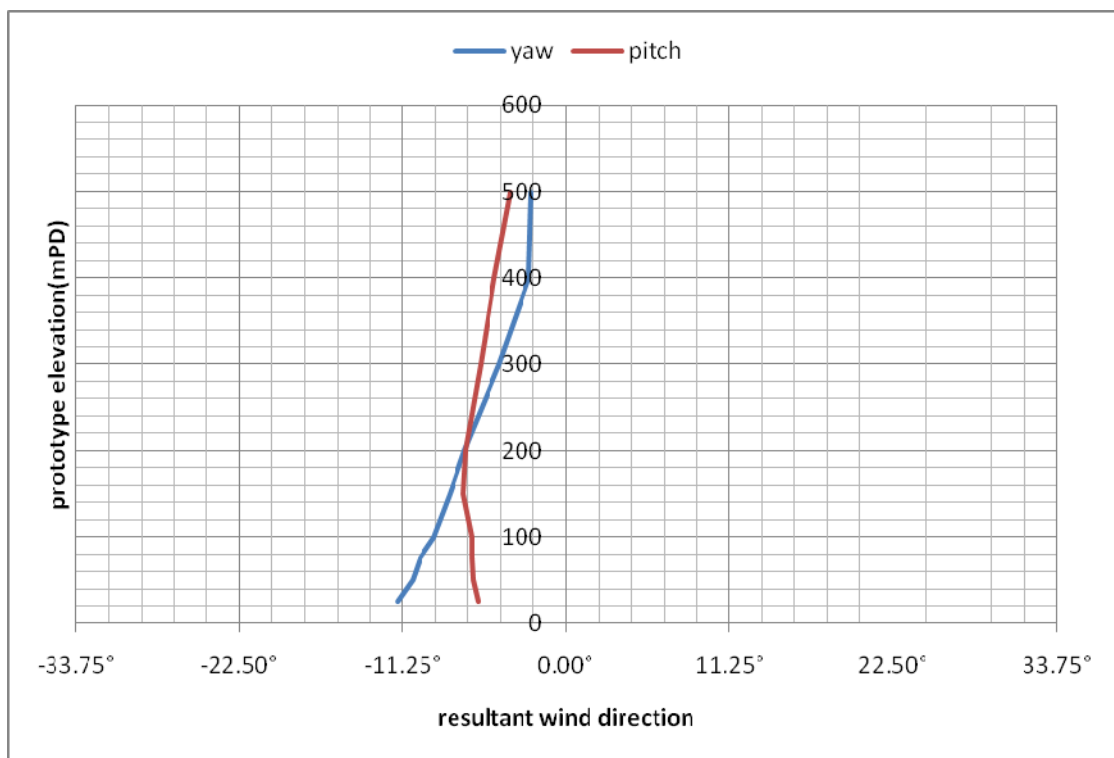


Figure 9b: Mean wind directions for San Po Kong, 22.5°

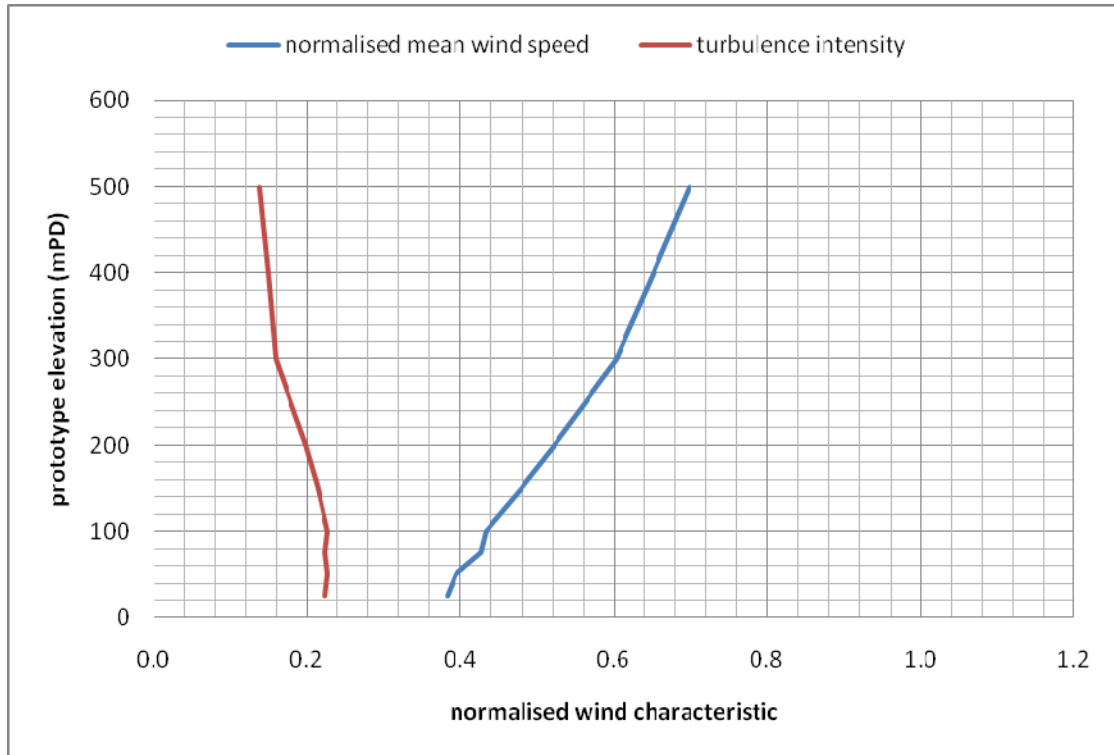


Figure 10a: Wind characteristics for San Po Kong, 45°

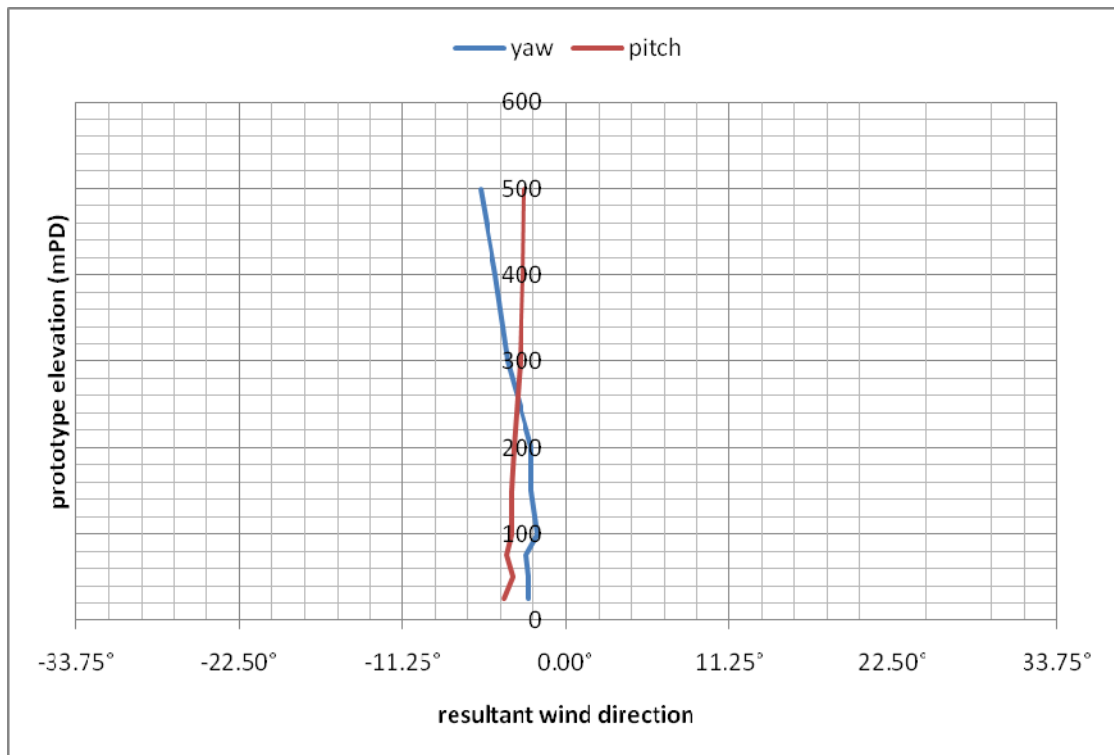


Figure 10b: Mean wind directions for San Po Kong, 45°

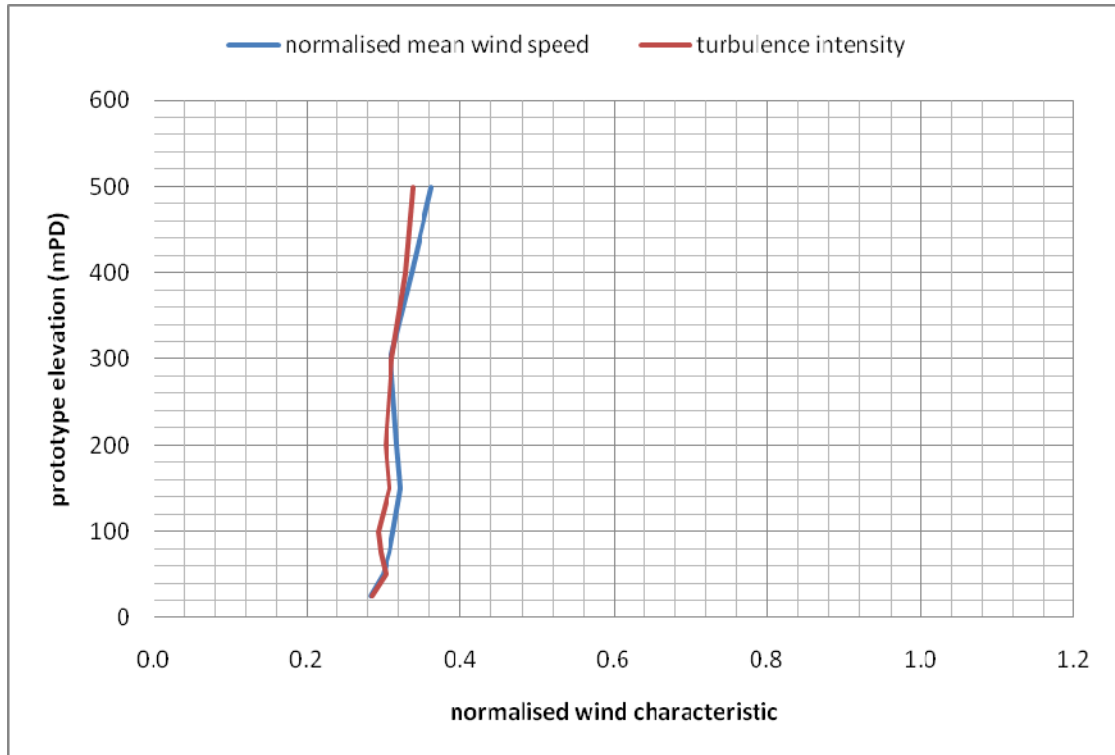


Figure 11a: Wind characteristics for San Po Kong, 67.5°

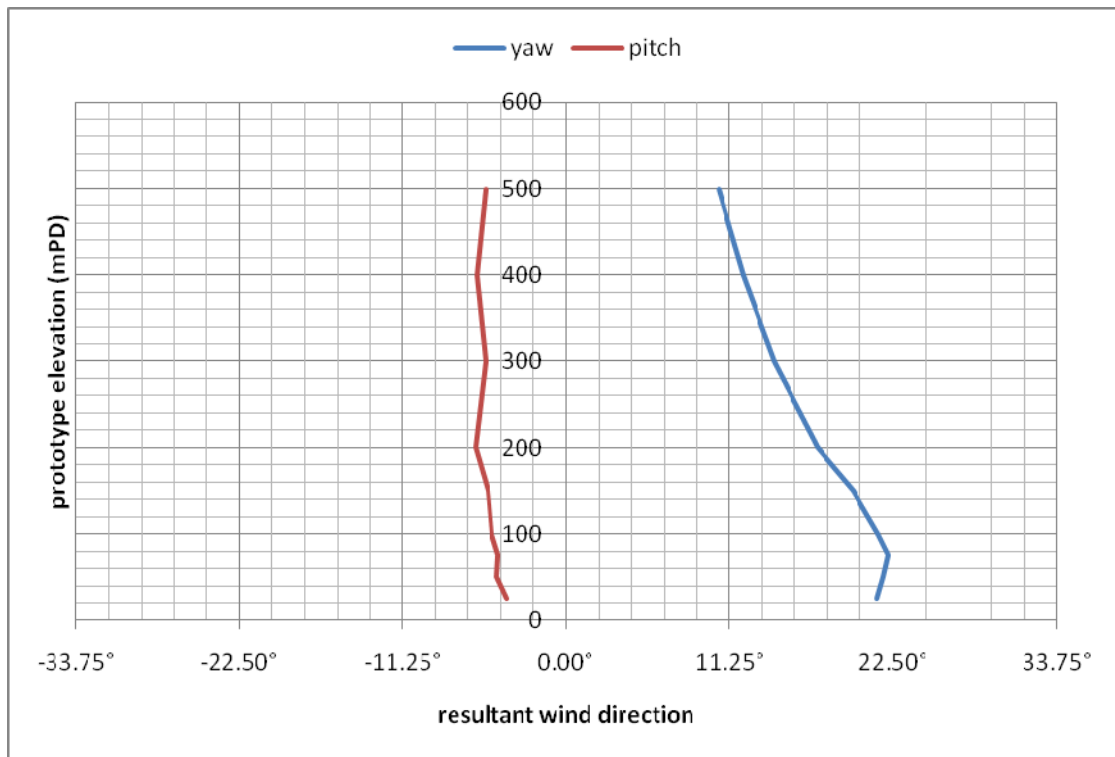


Figure 11b: Mean wind directions for San Po Kong, 67.5°

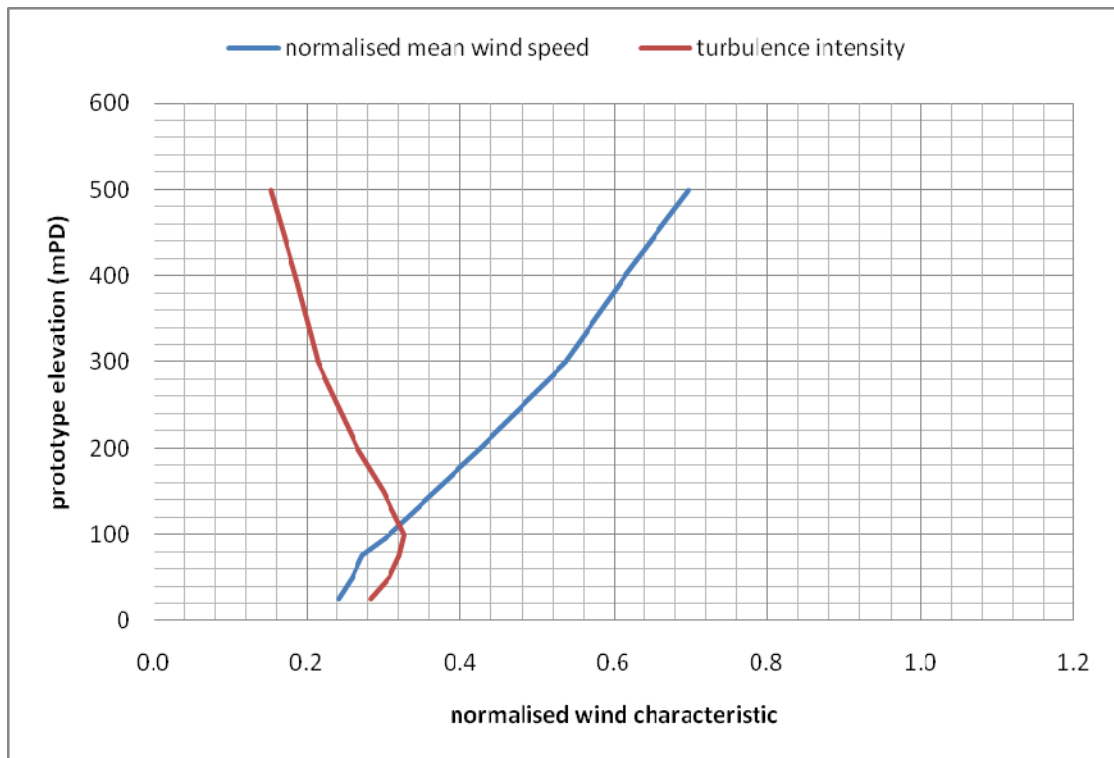


Figure 12a: Wind characteristics for San Po Kong, 90°

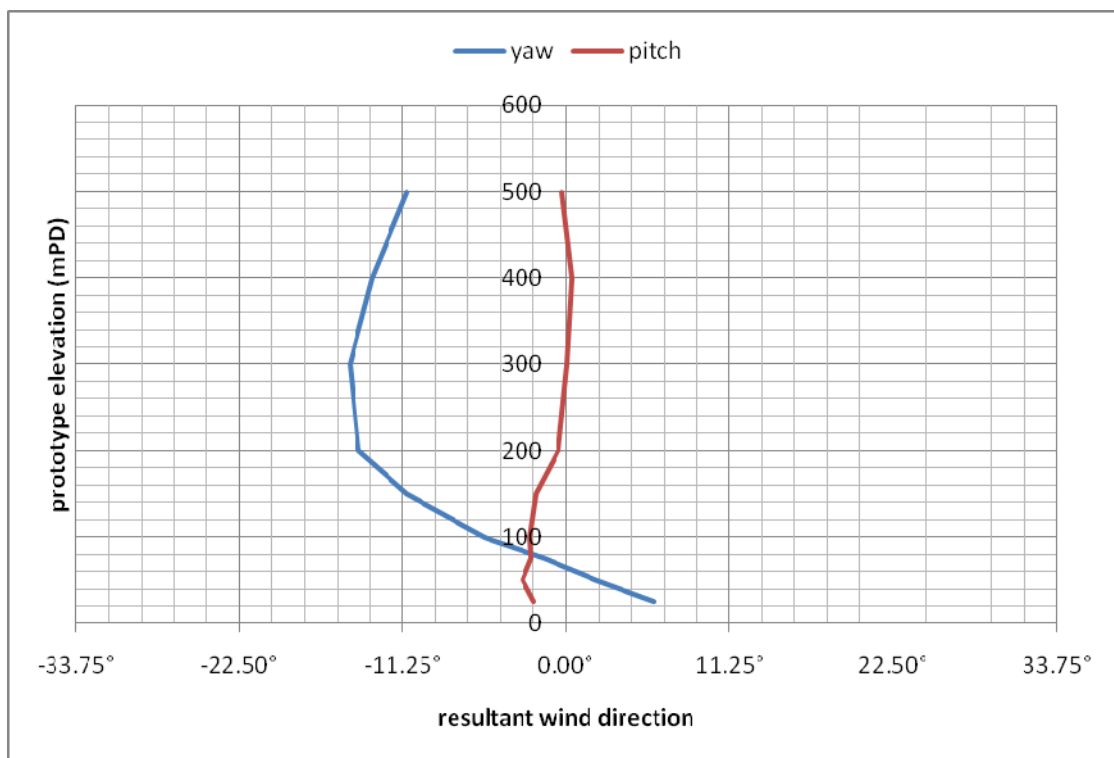


Figure 12b: Mean wind directions for San Po Kong, 90°

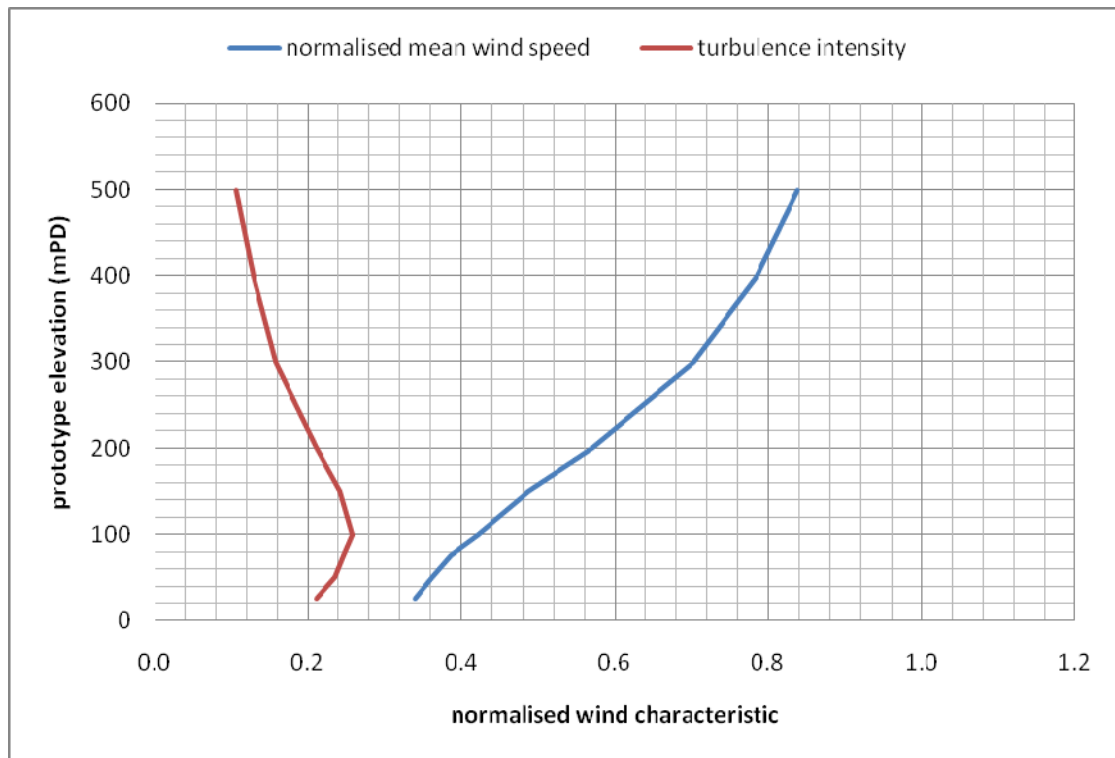


Figure 13a: Wind characteristics for San Po Kong, 112.5°

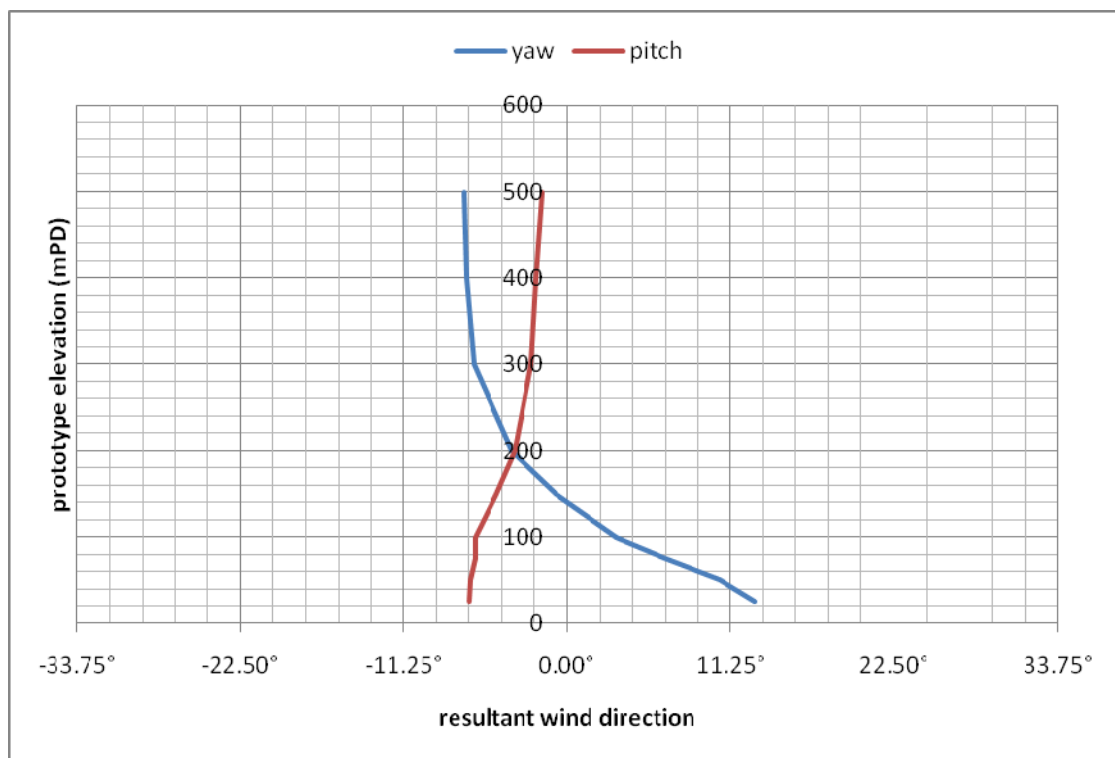


Figure 13b: Mean wind directions for San Po Kong, 112.5°

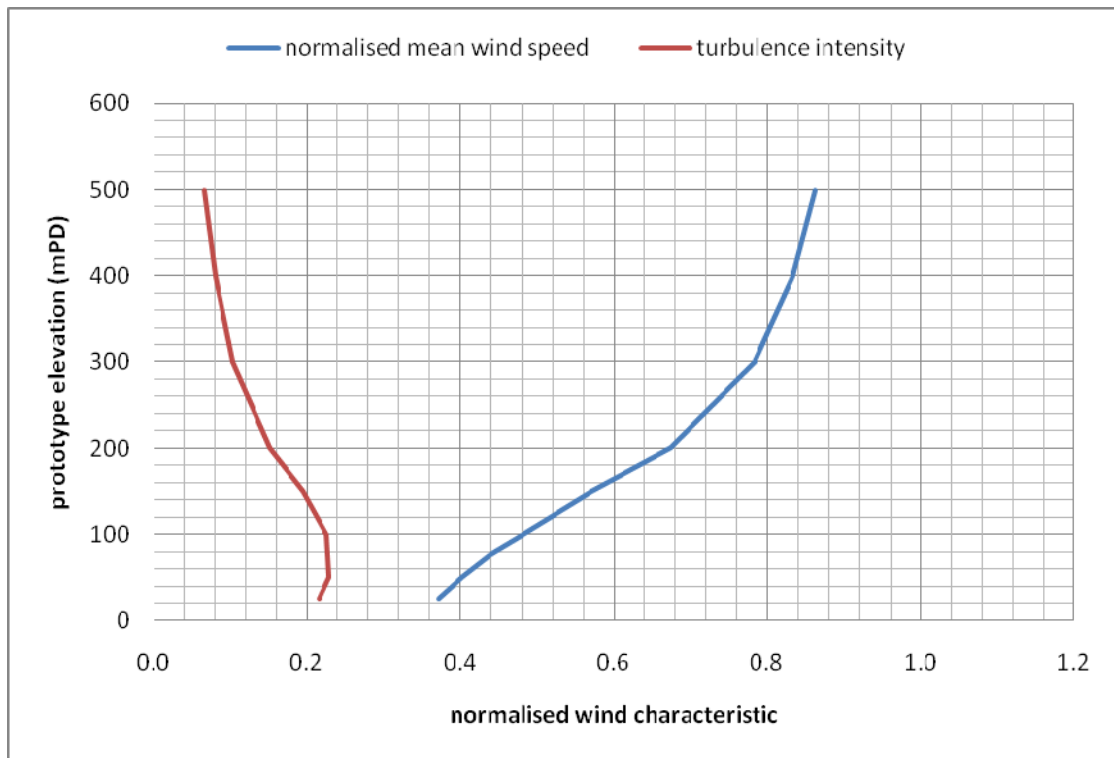


Figure 14a: Wind characteristics for San Po Kong, 135°

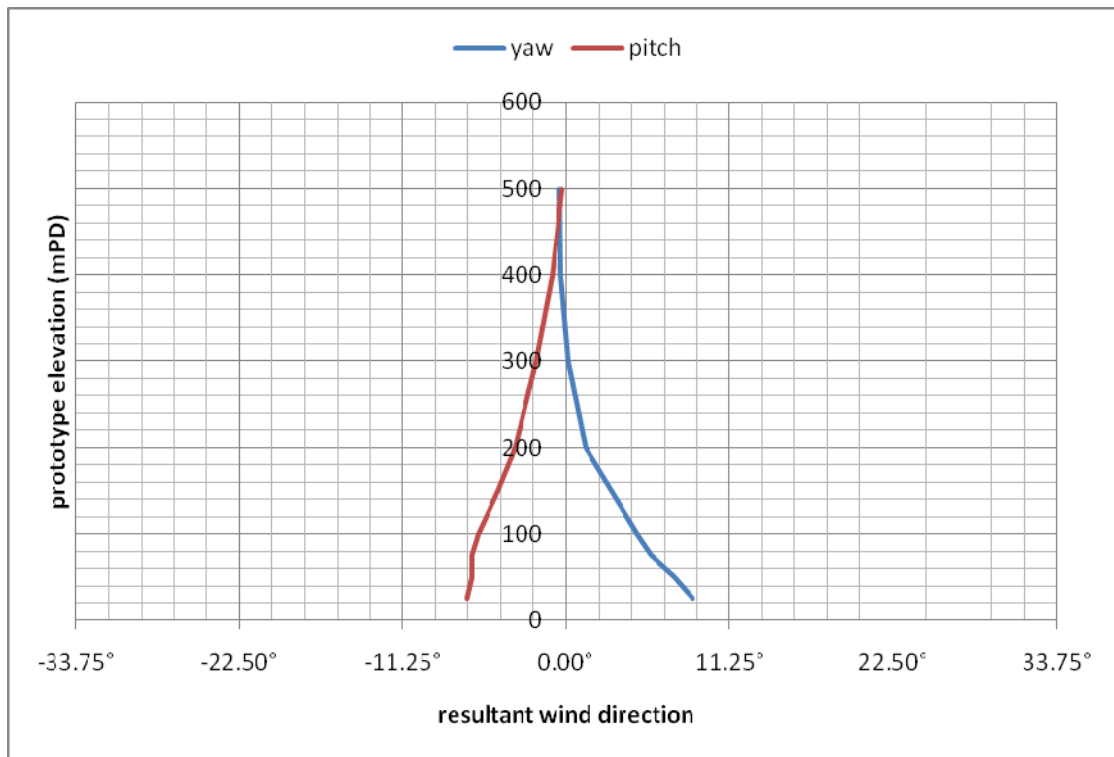


Figure 14b: Mean wind directions for San Po Kong, 135°

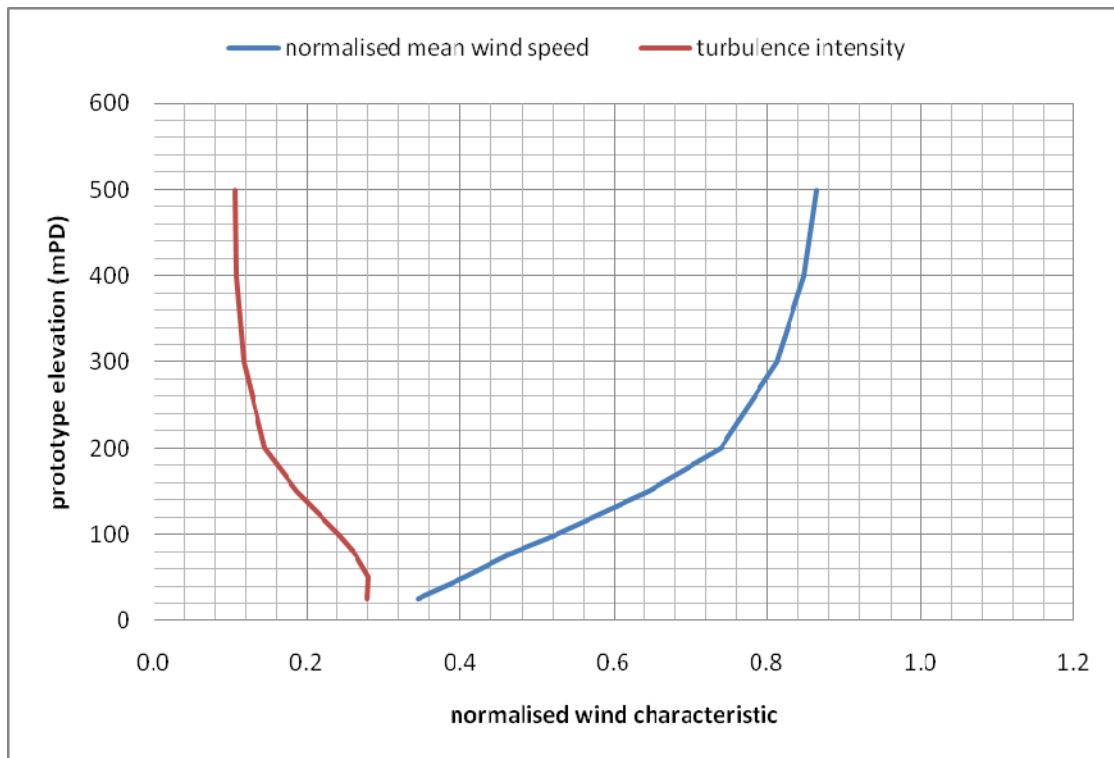


Figure 15a: Wind characteristics for San Po Kong, 157.5°

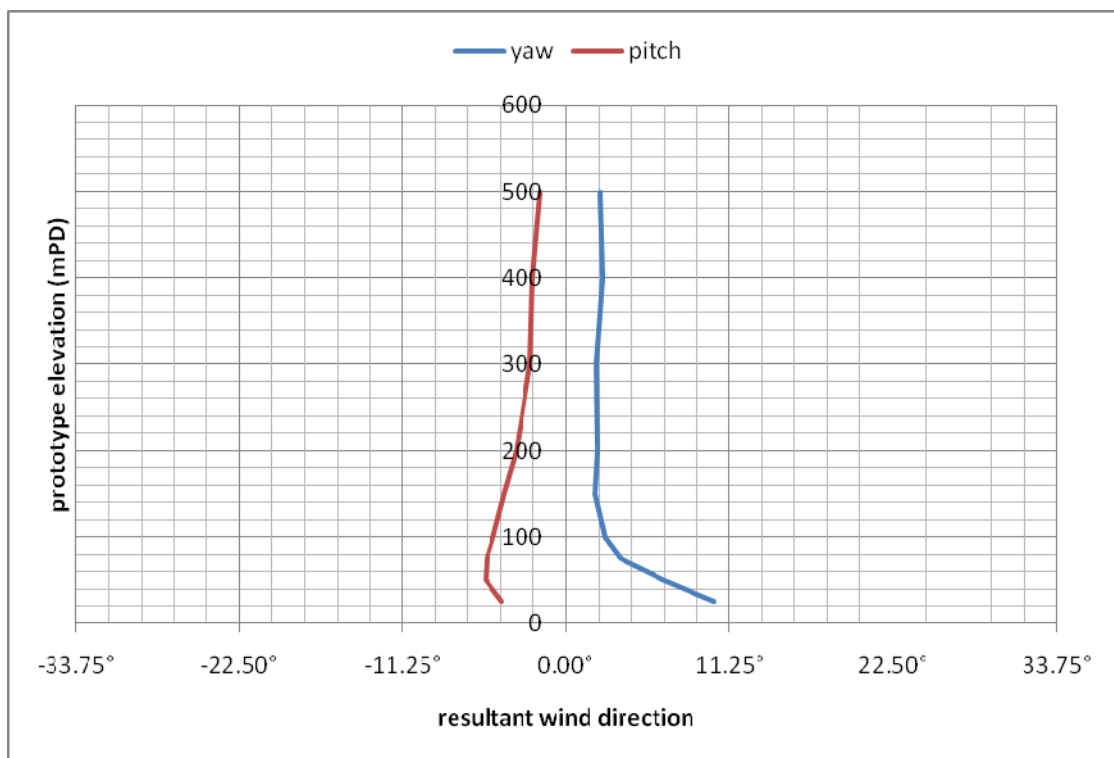


Figure 15b: Mean wind directions for San Po Kong, 157.5°

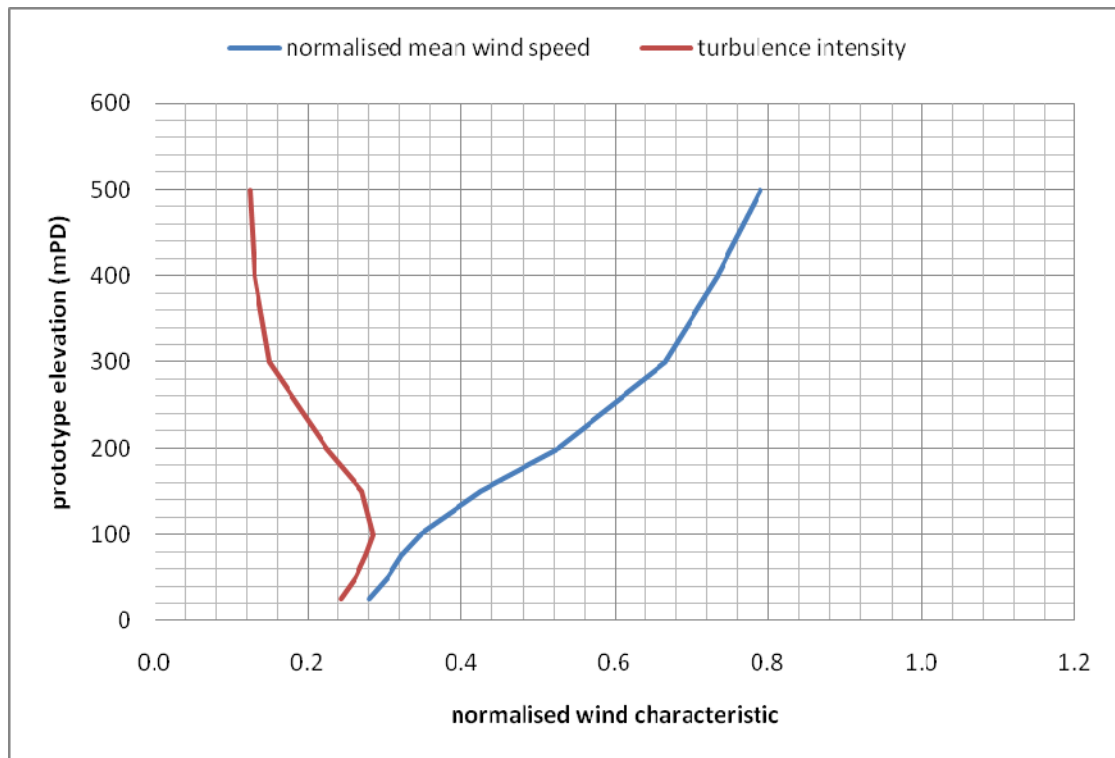


Figure 16a: Wind characteristics for San Po Kong, 180°

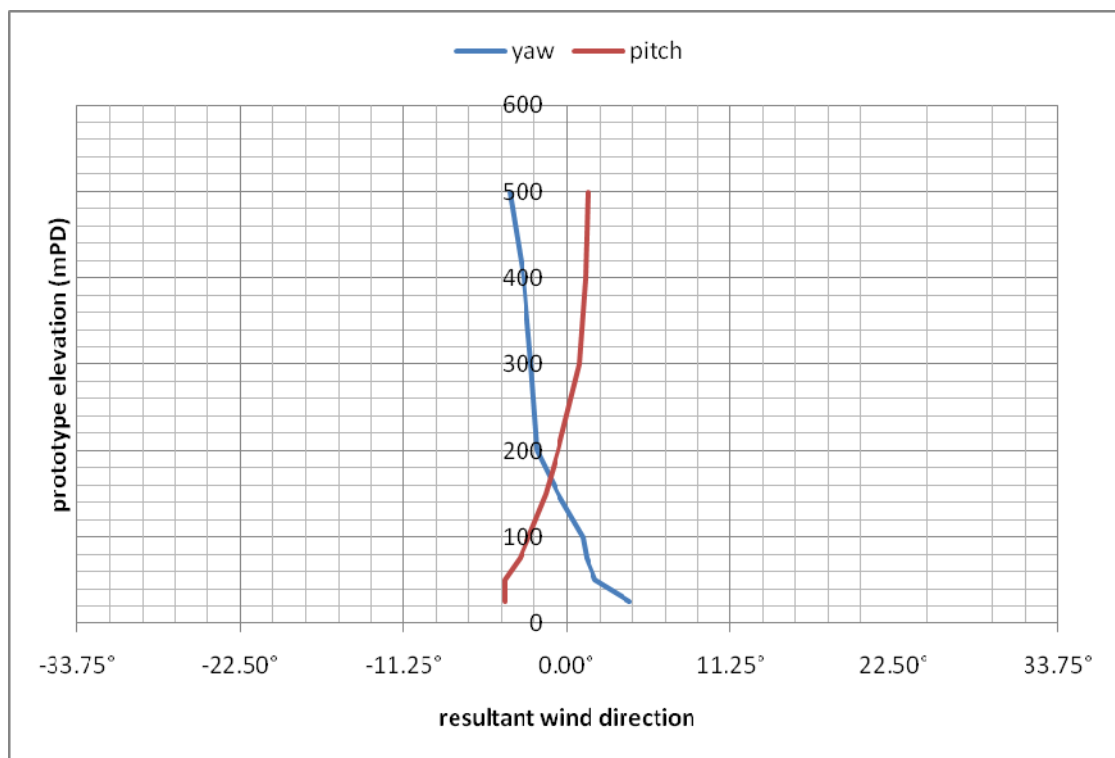


Figure 16b: Mean wind directions for San Po Kong, 180°

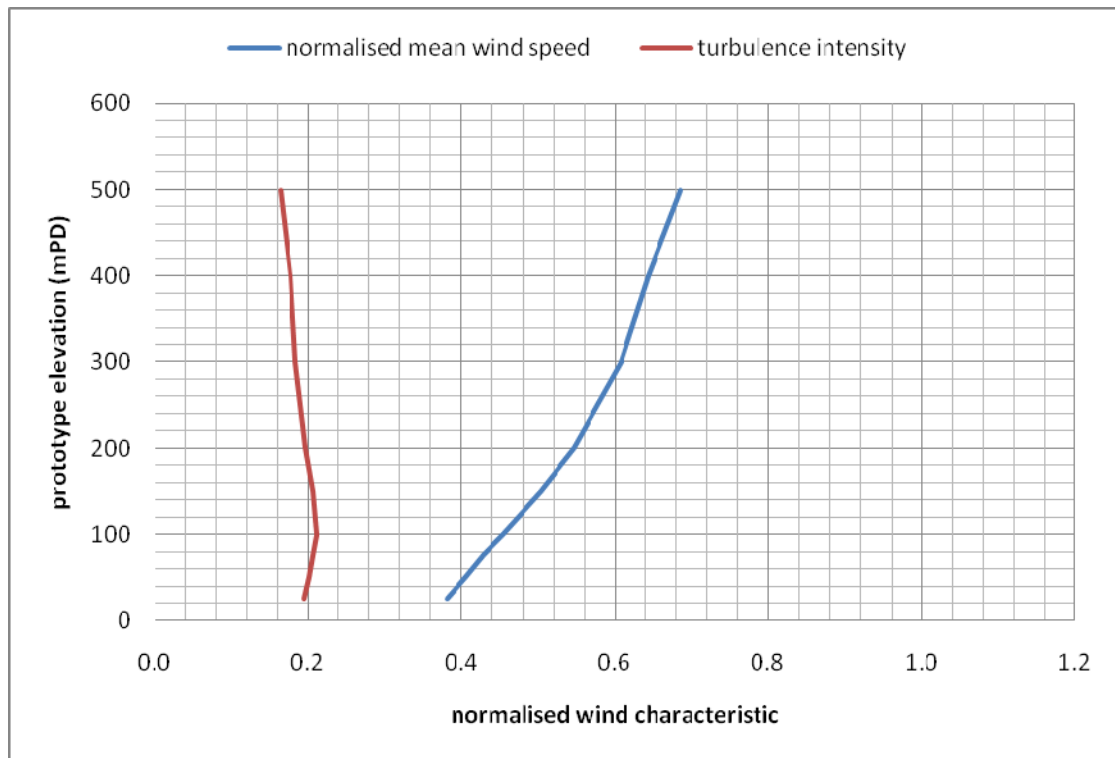


Figure 17a: Wind characteristics for San Po Kong, 202.5°

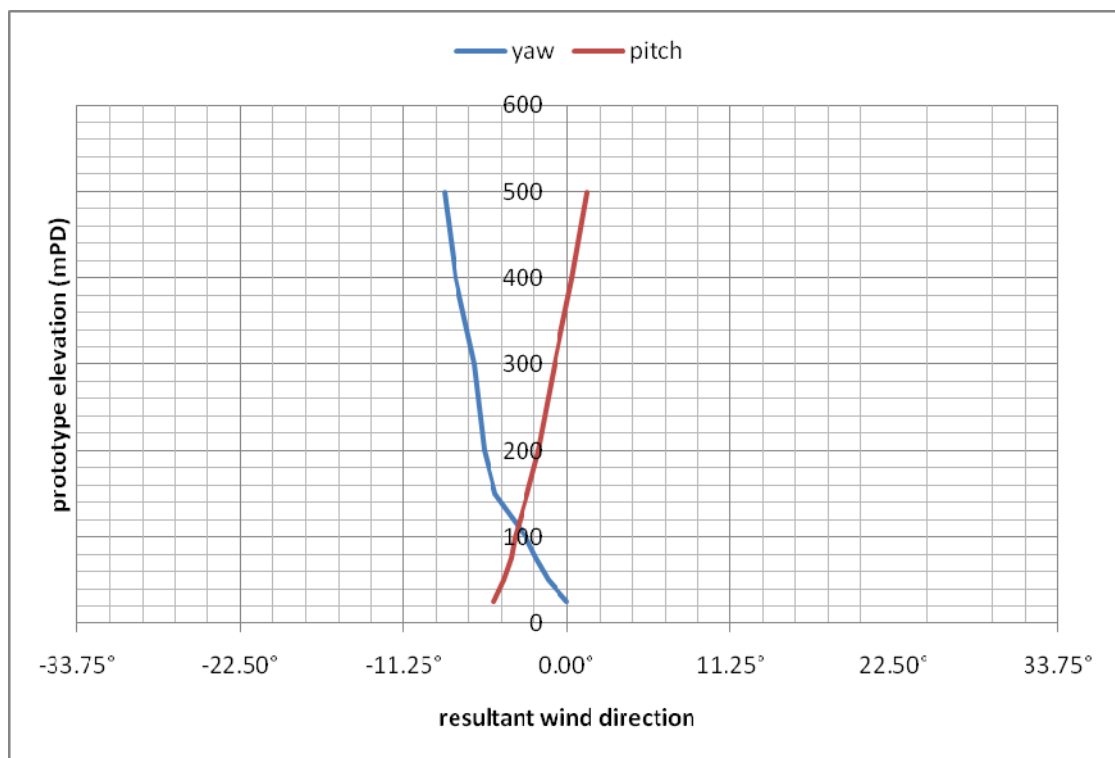


Figure 17b: Mean wind directions for San Po Kong, 202.5°

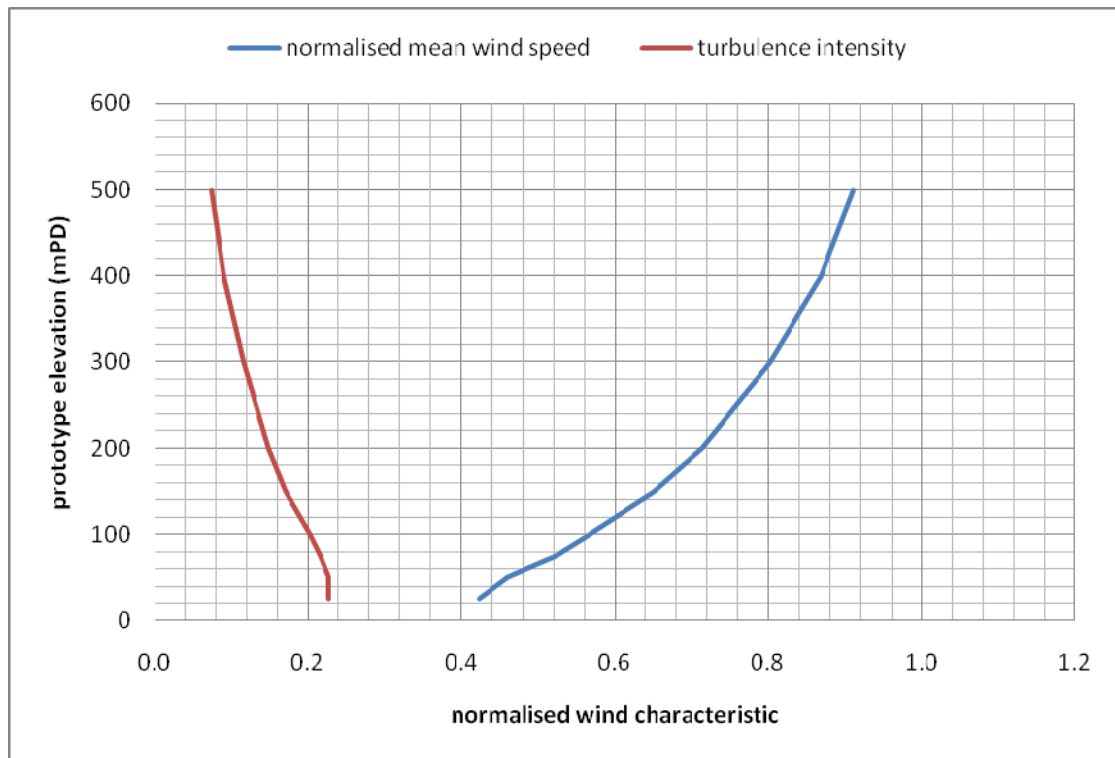


Figure 18a: Wind characteristics for San Po Kong, 225°

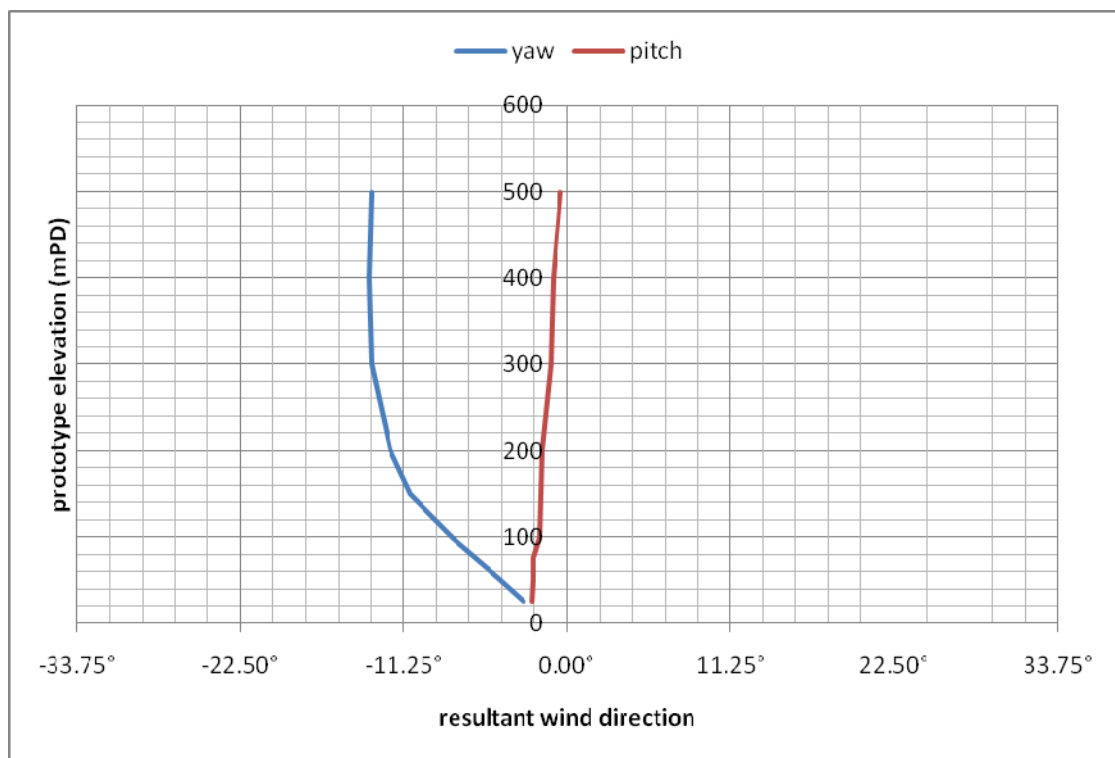


Figure 18b: Mean wind directions for San Po Kong, 225°

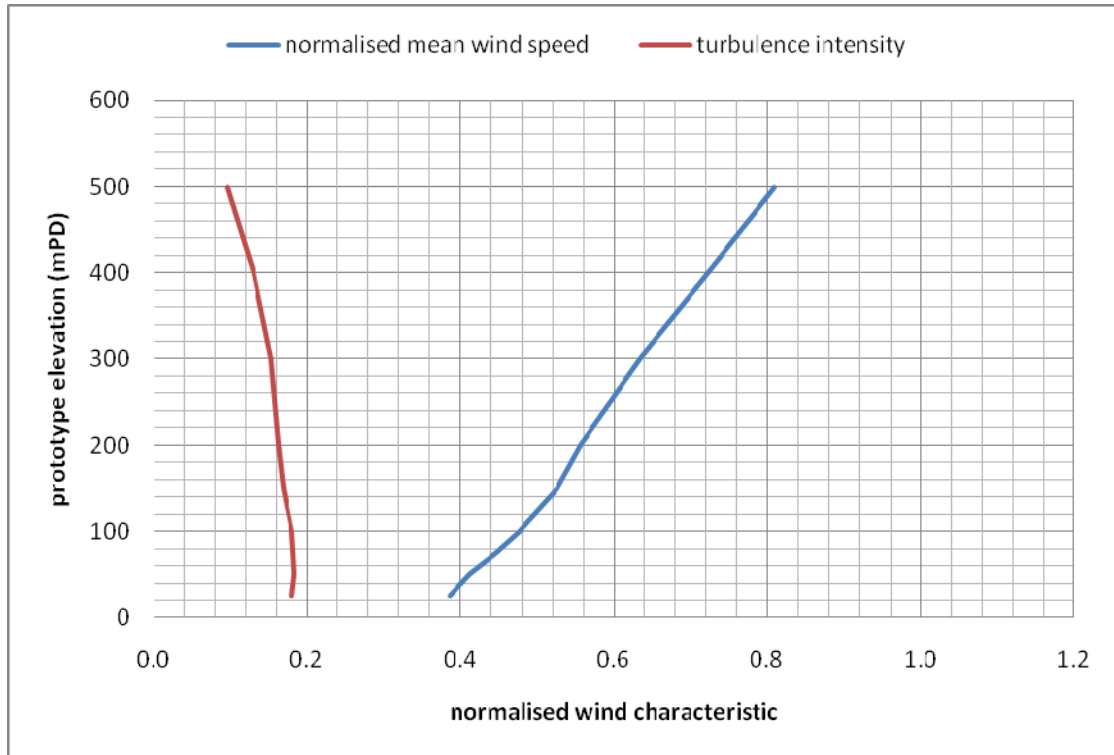


Figure 19a: Wind characteristics for San Po Kong, 247.5°

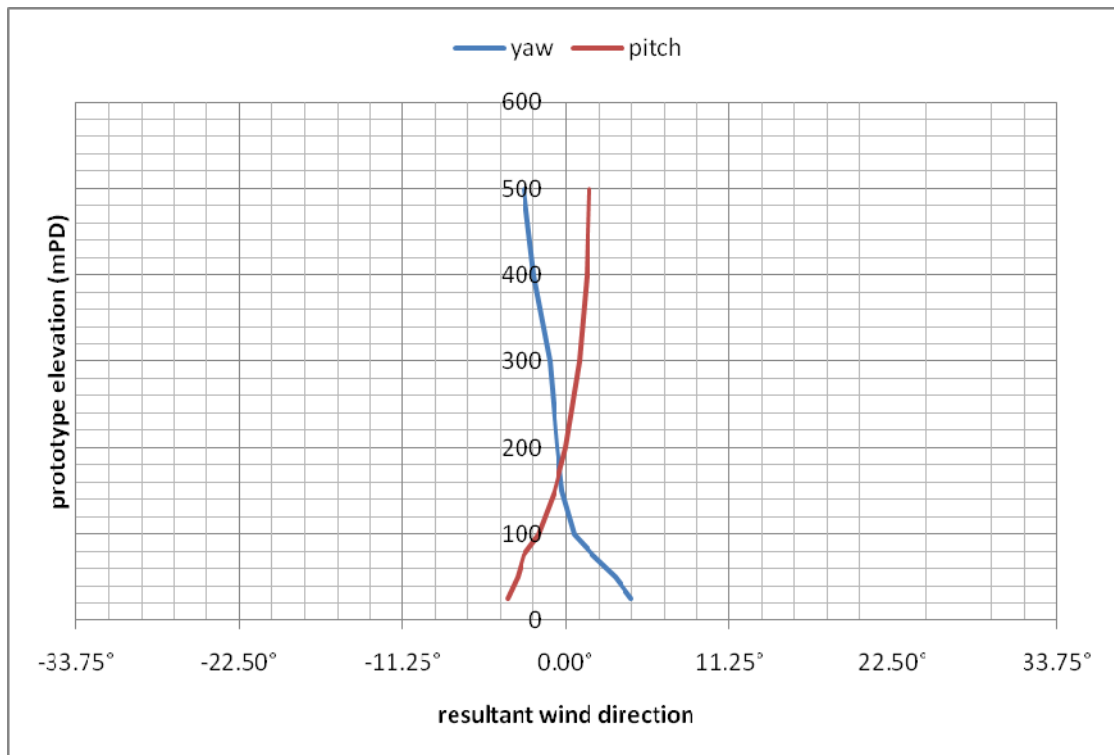


Figure 19b: Mean wind directions for San Po Kong, 247.5°

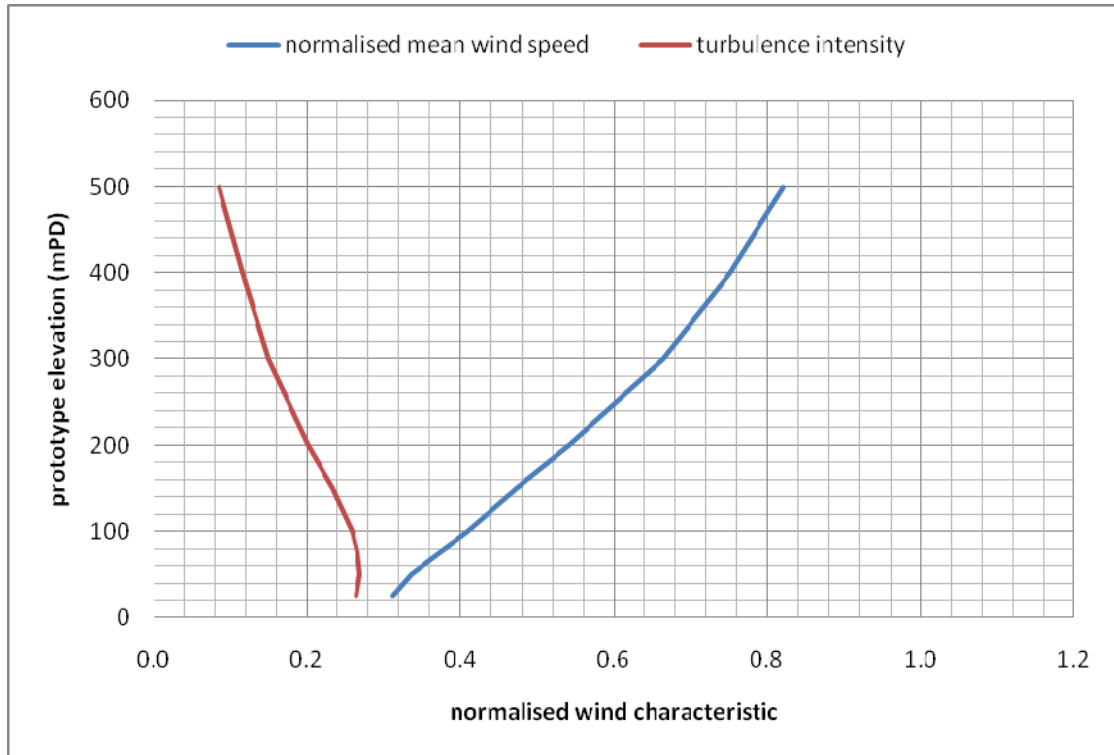


Figure 20a: Wind characteristics for San Po Kong, 270°

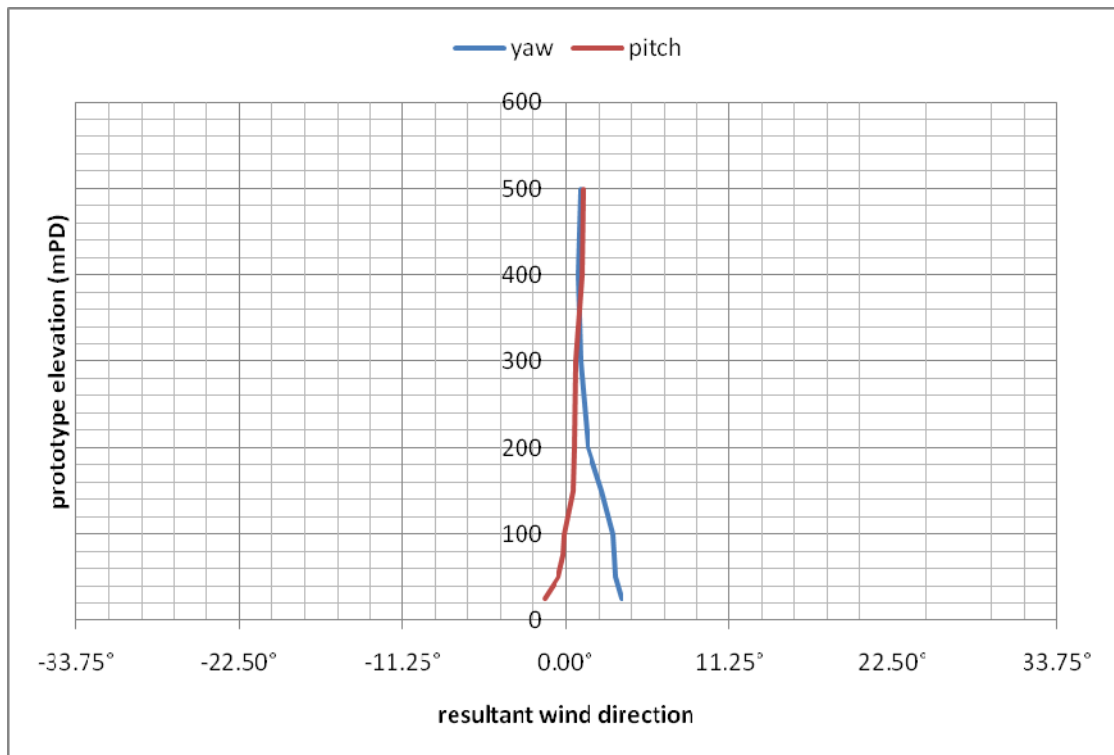


Figure 20b: Mean wind directions for San Po Kong, 270°

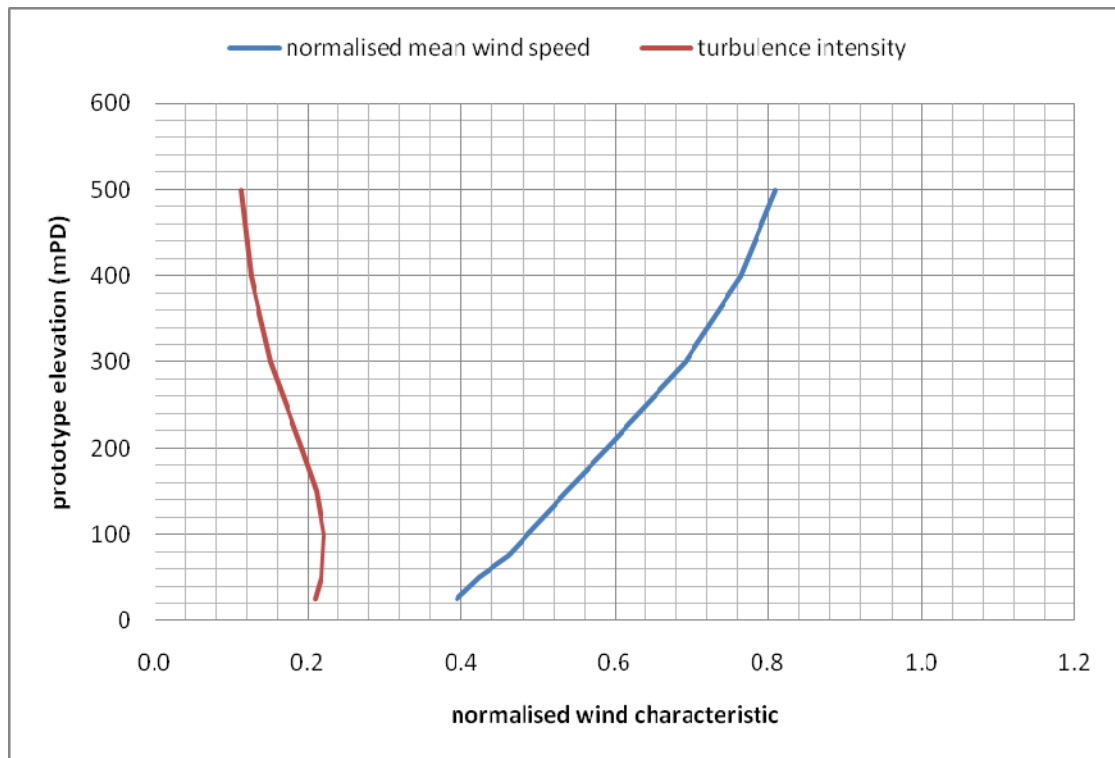


Figure 21a: Wind characteristics for San Po Kong, 292.5°

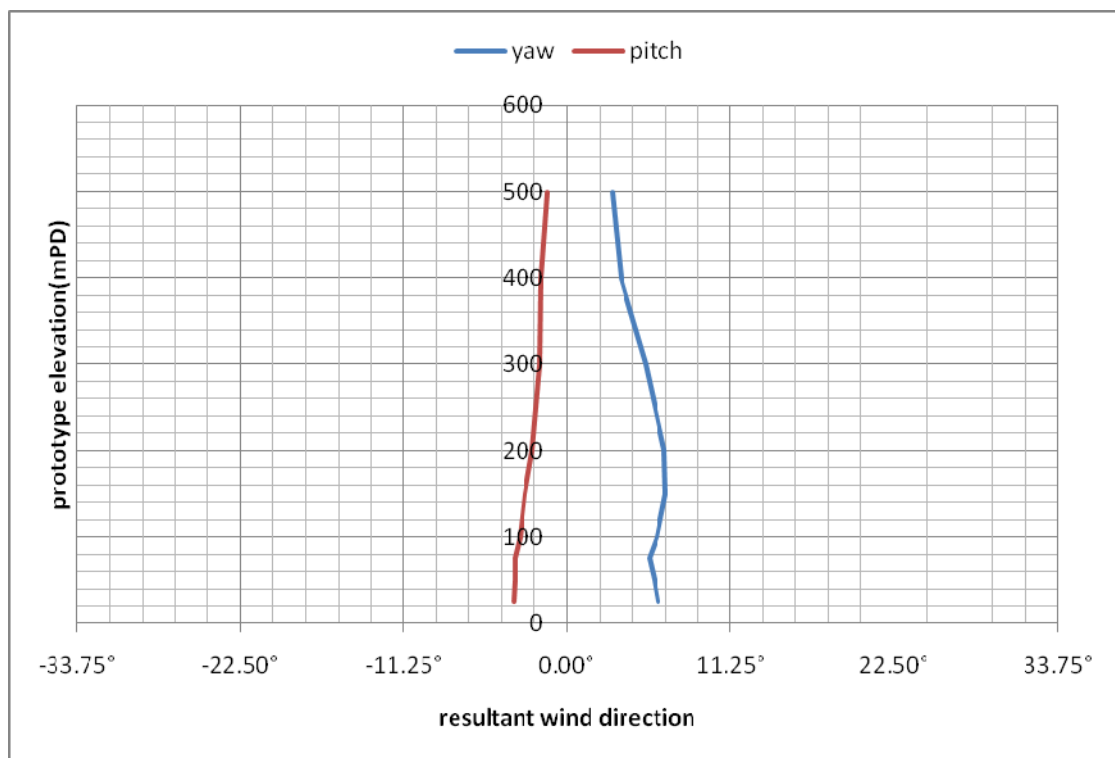


Figure 21b: Mean wind directions for San Po Kong, 292.5°

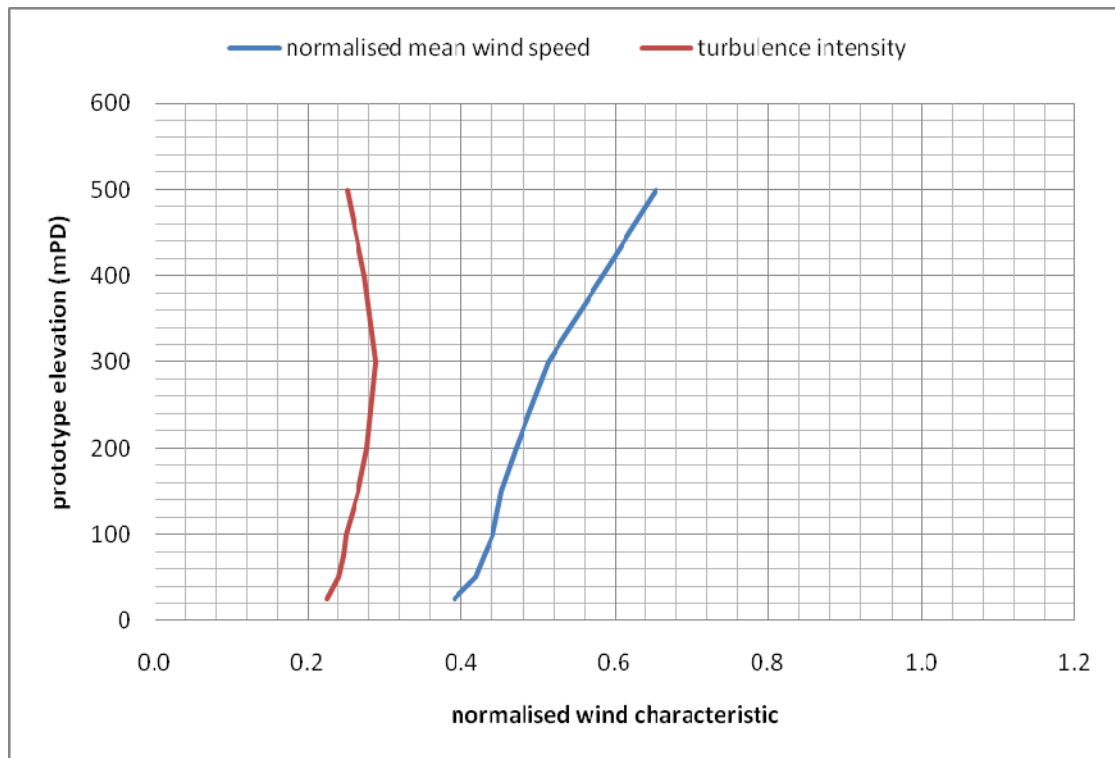


Figure 22a: Wind characteristics for San Po Kong, 315°

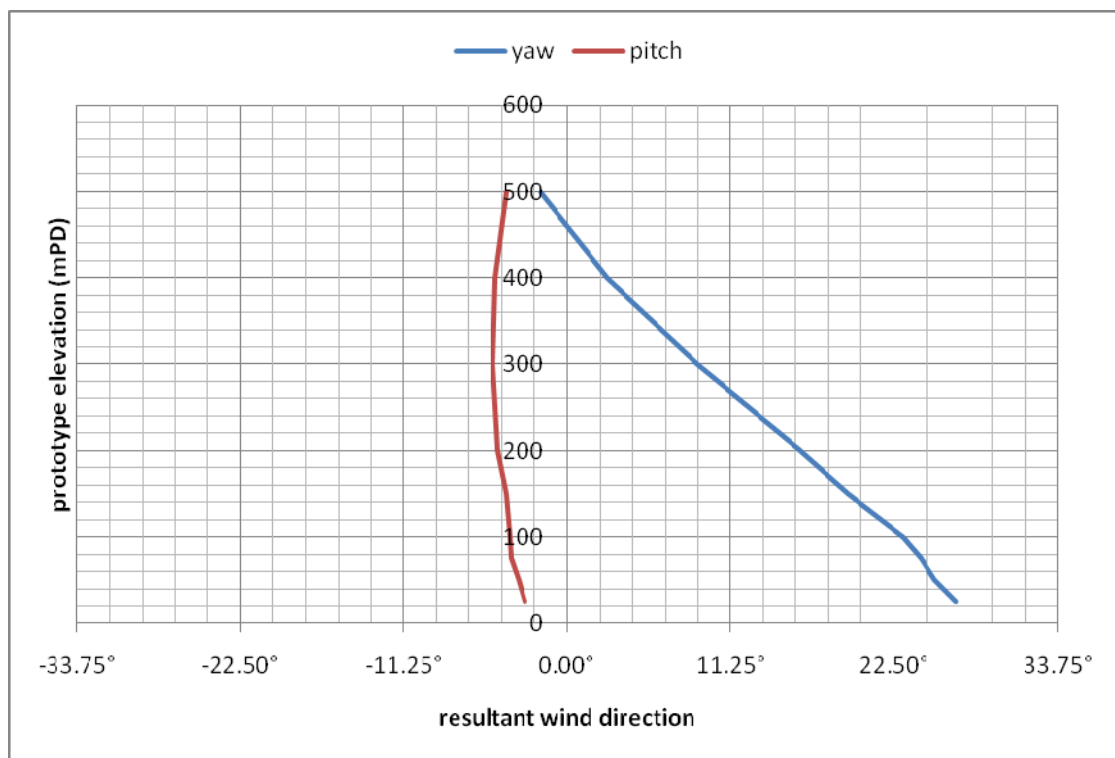


Figure 22b: Mean wind directions for San Po Kong, 315°

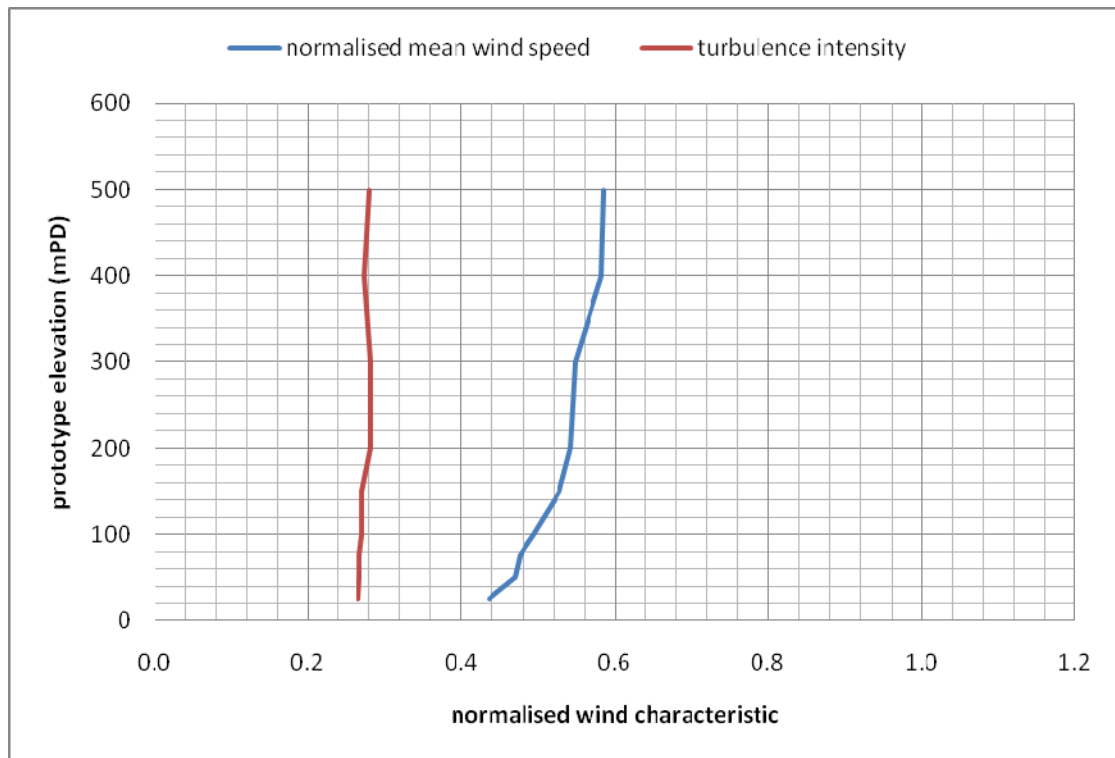


Figure 23a: Wind characteristics for San Po Kong, 337.5°

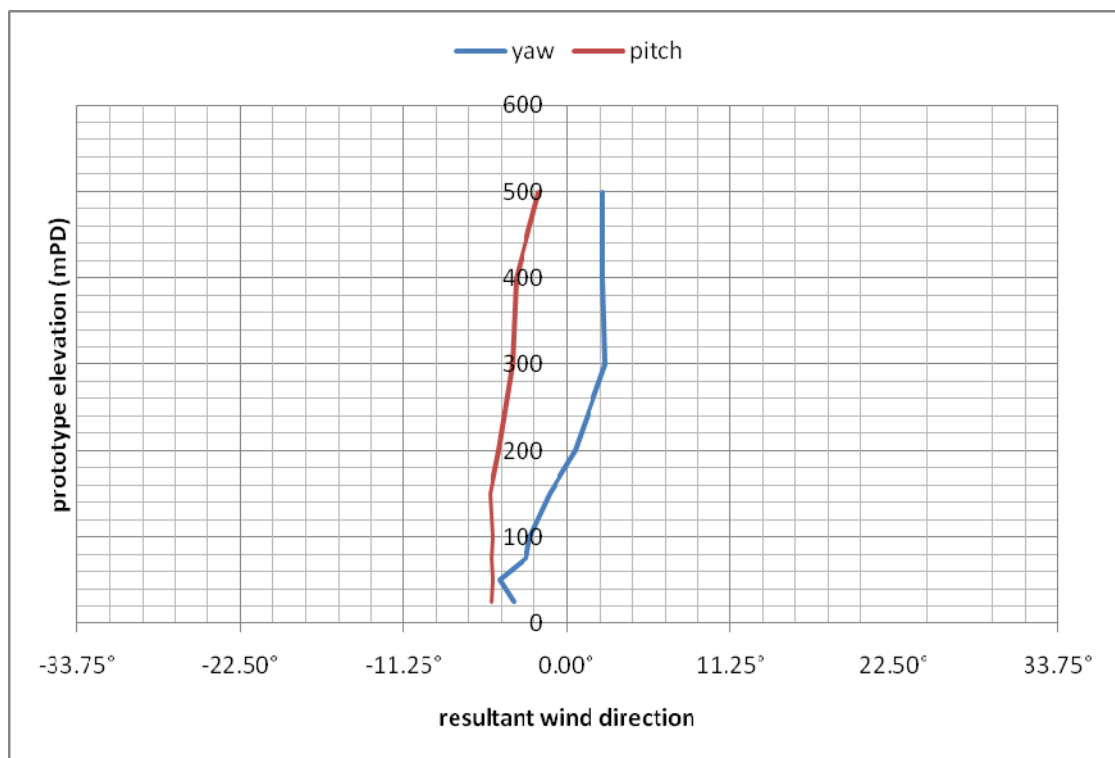


Figure 23b: Mean wind directions for San Po Kong, 337.5°

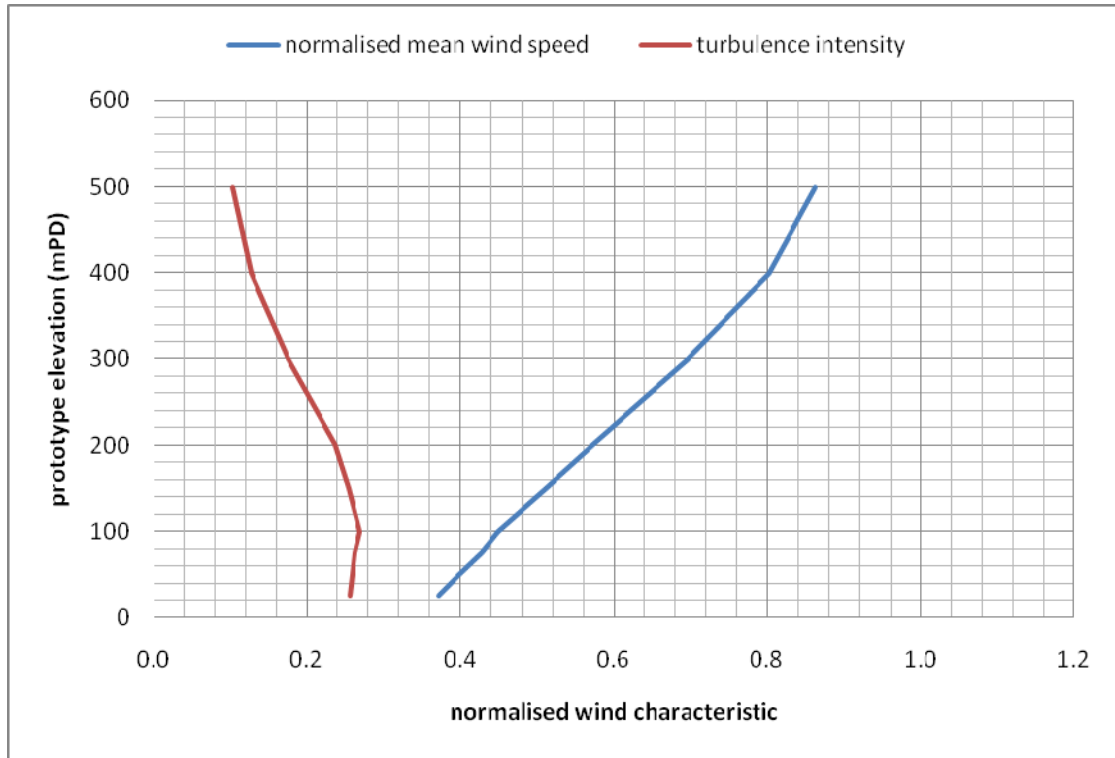


Figure 24a: Wind characteristics for San Po Kong, 360°

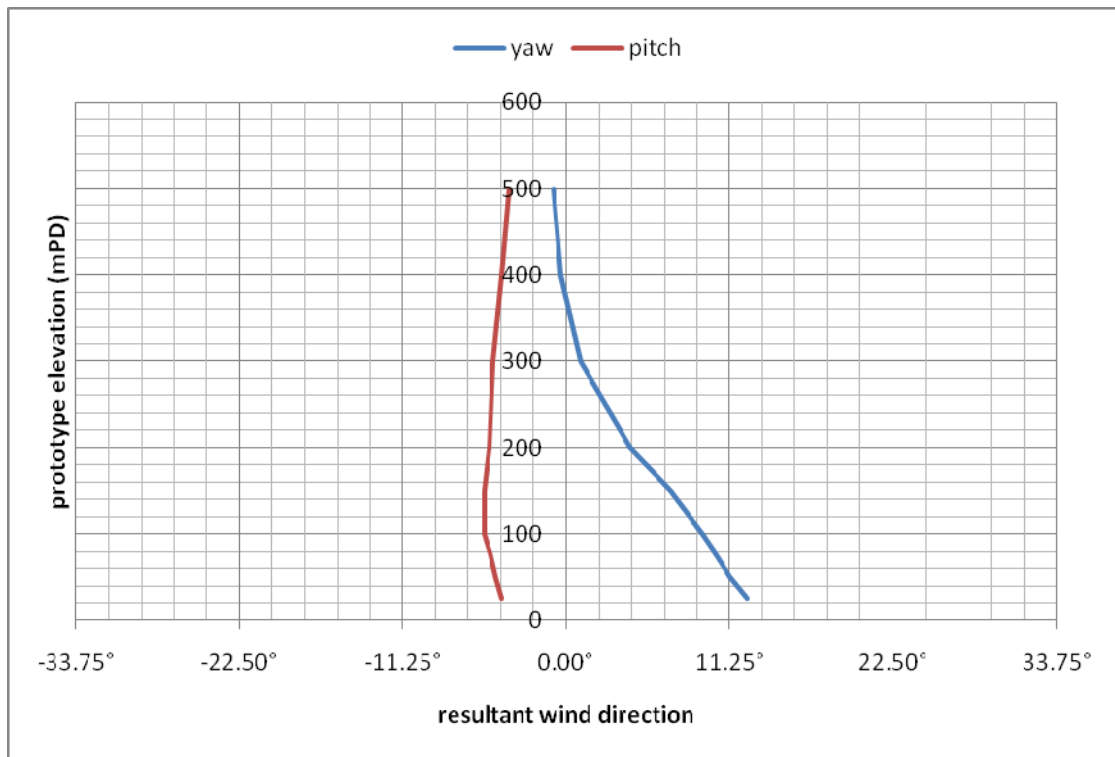


Figure 24b: Mean wind directions for San Po Kong, 360°

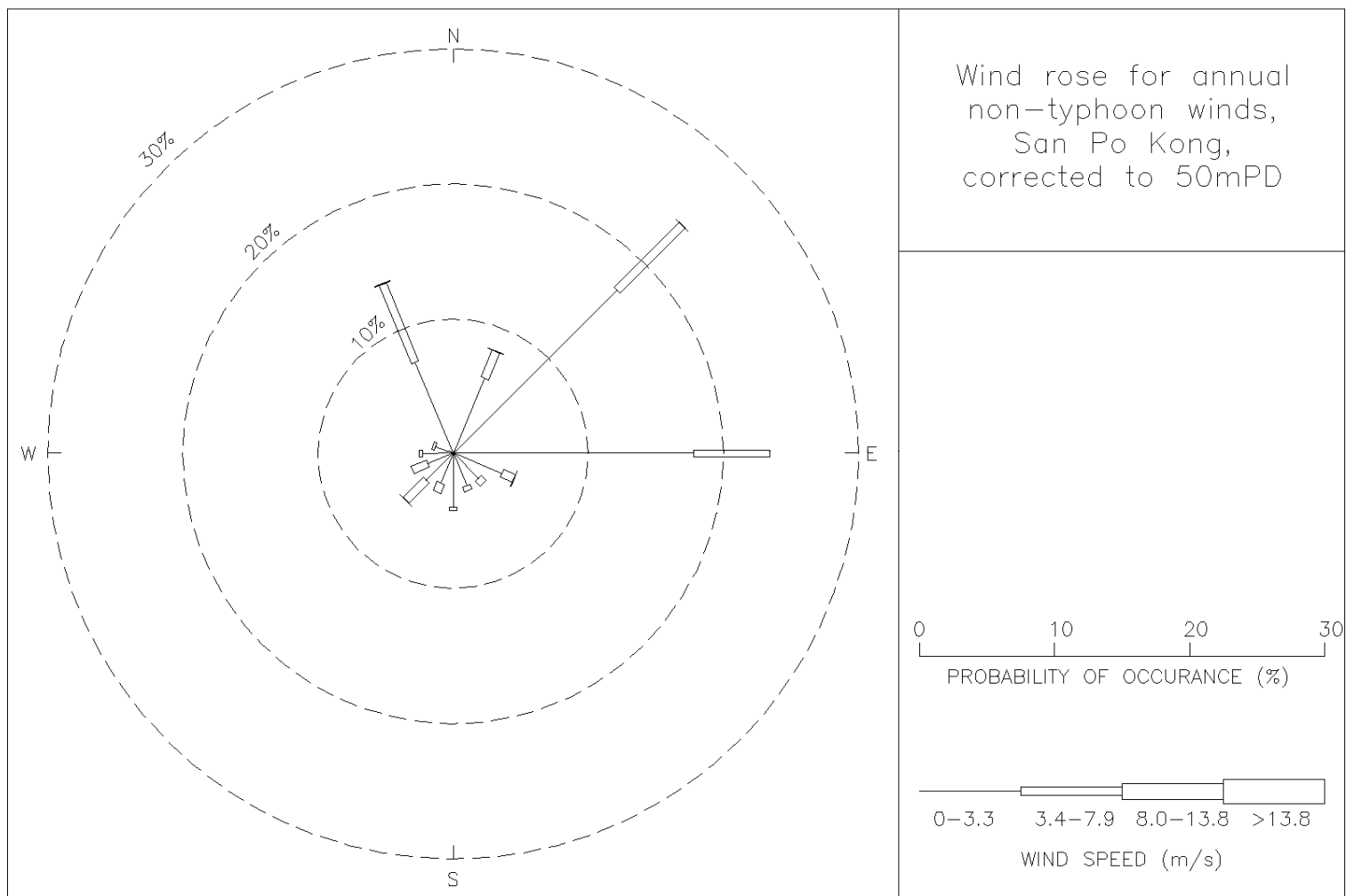


Figure 25: Wind rose for annual, non-typhoon winds for San Po Kong, corrected to 50 mPD

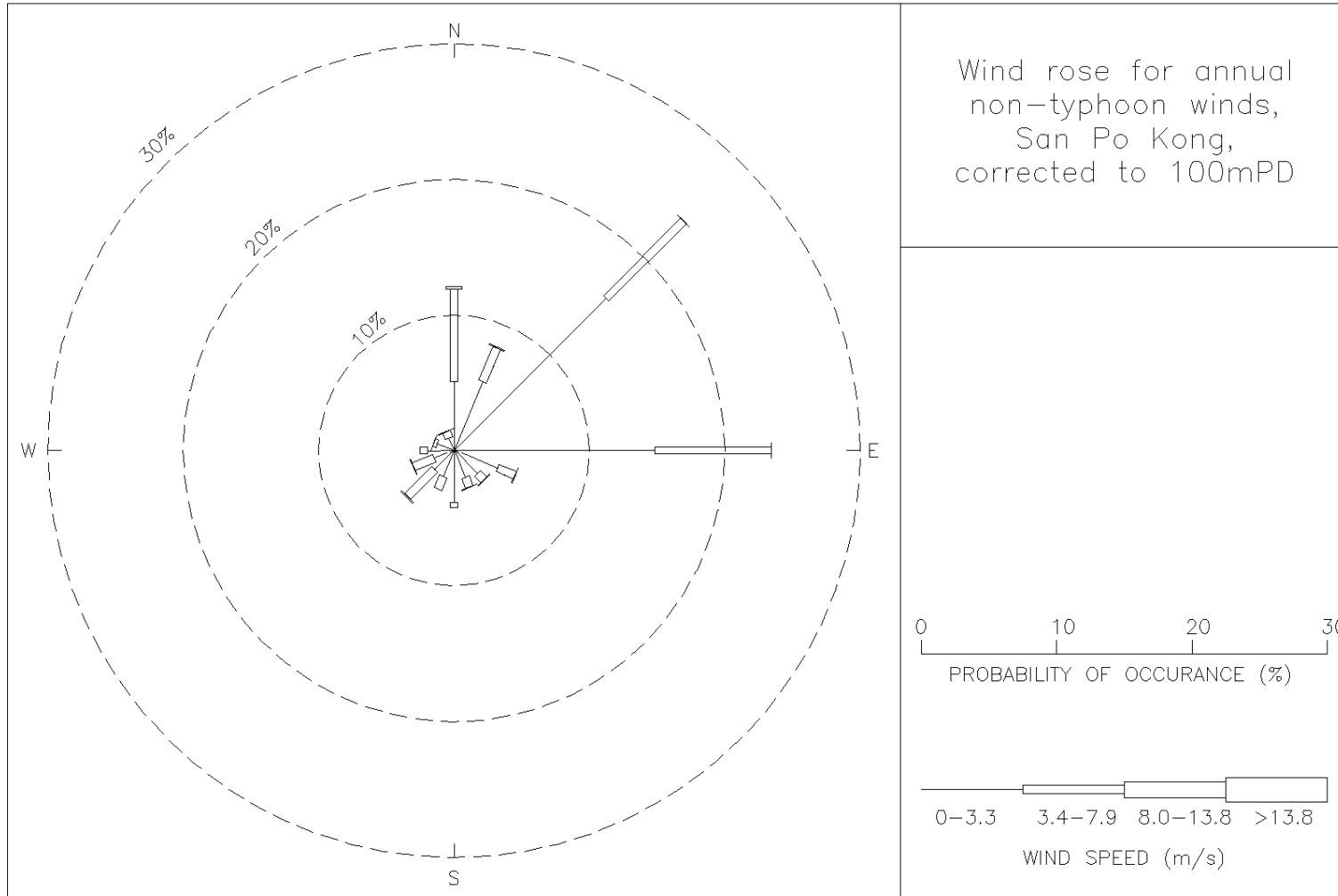


Figure 26: Wind rose for annual, non-typhoon winds for San Po Kong, corrected to 100 mPD

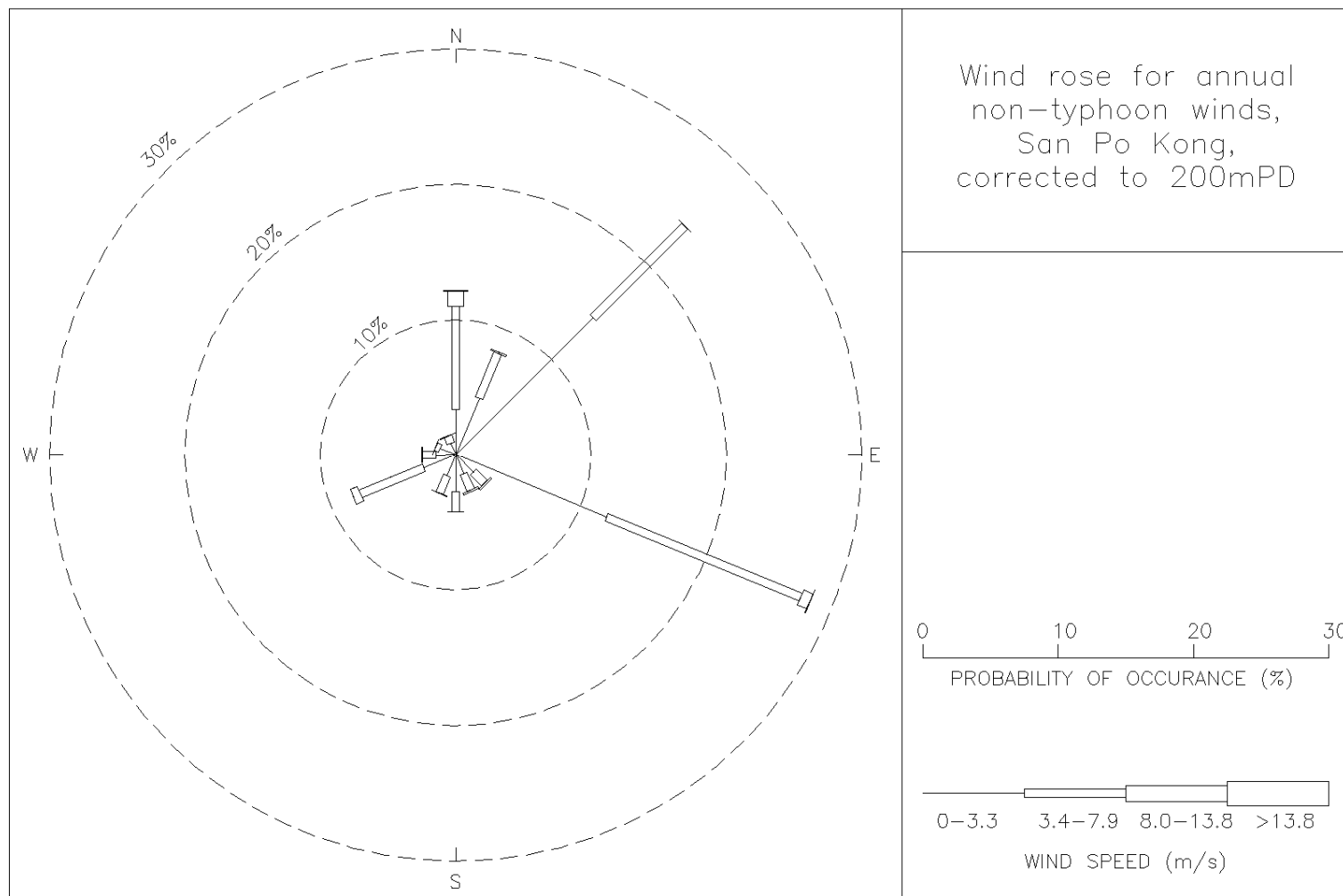


Figure 27: Wind rose for annual, non-typhoon winds for San Po Kong, corrected to 200 mPD

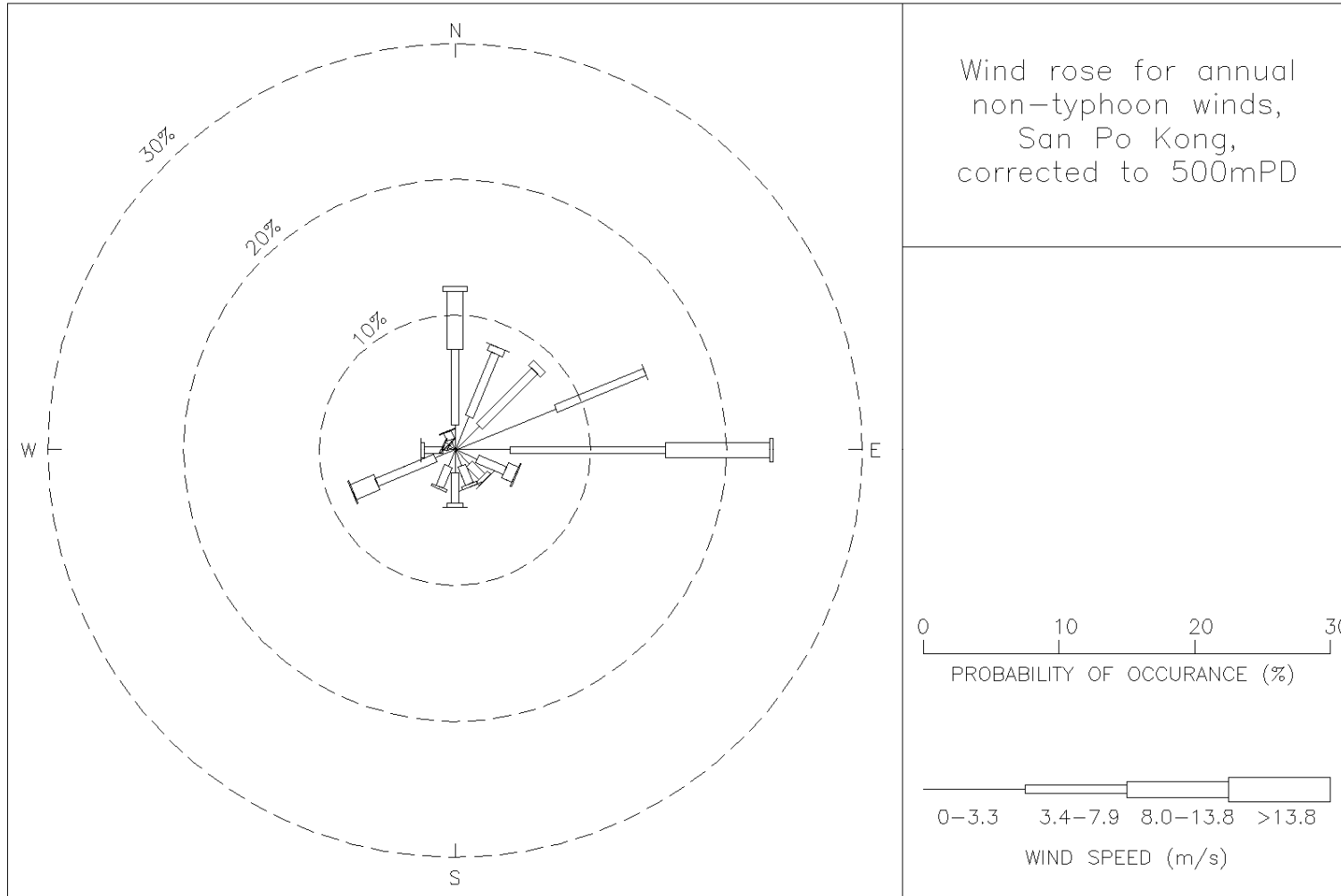


Figure 28: Wind rose for annual, non-typhoon winds for San Po Kong, corrected to 500 mPD

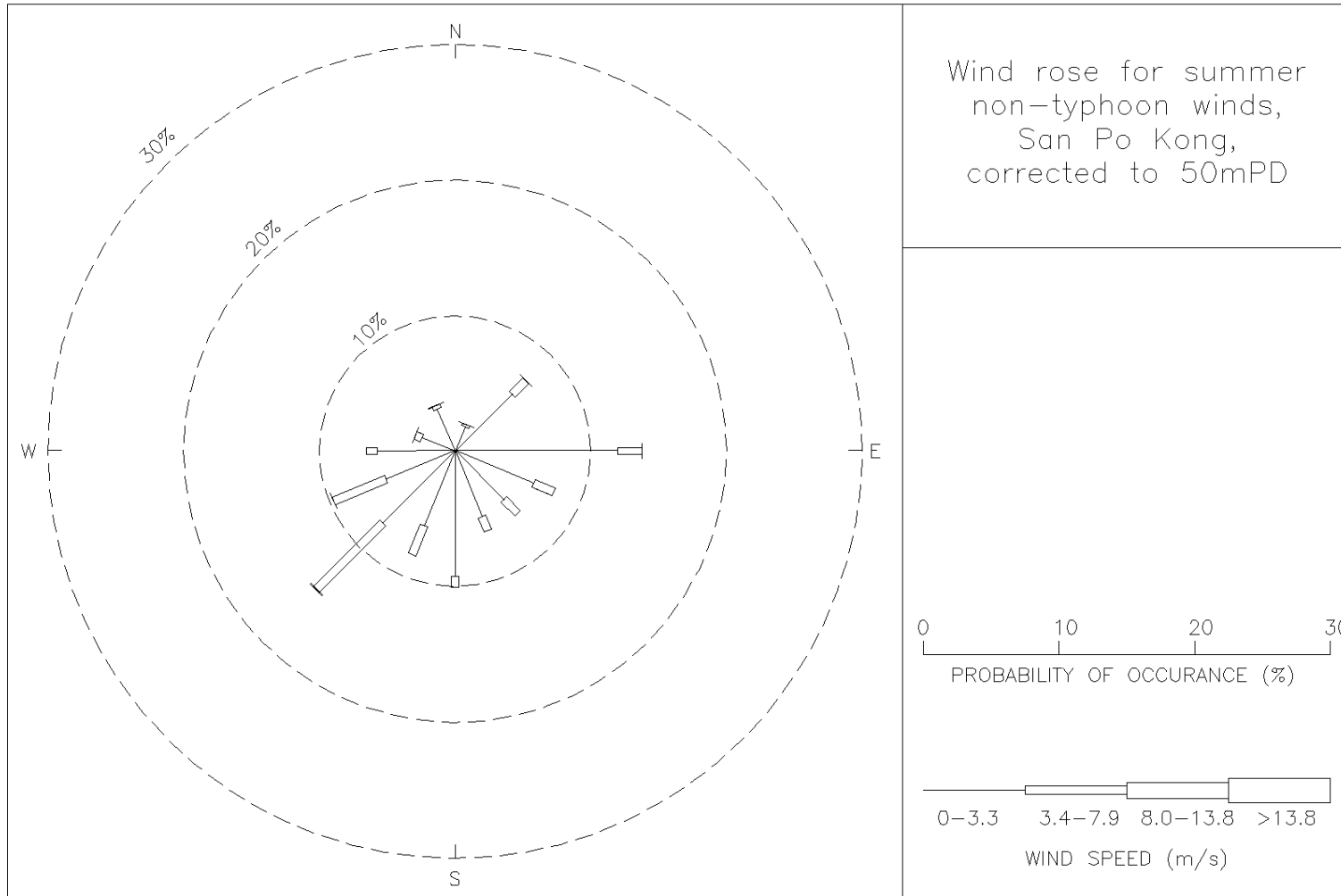


Figure 29: Wind rose for summer, non-typhoon winds for San Po Kong, corrected to 50 mPD

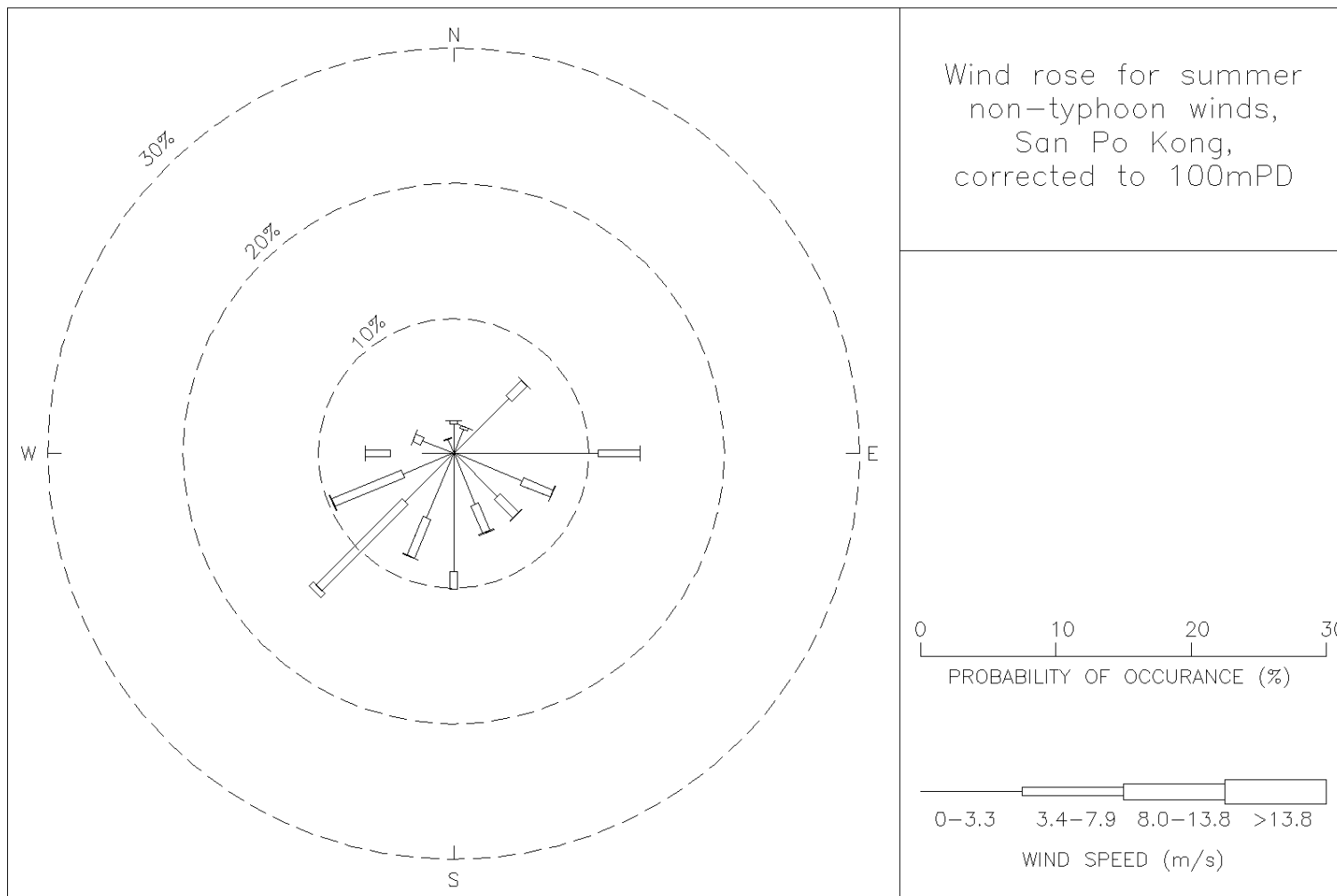


Figure 30: Wind rose for summer, non-typhoon winds for San Po Kong, corrected to 100 mPD

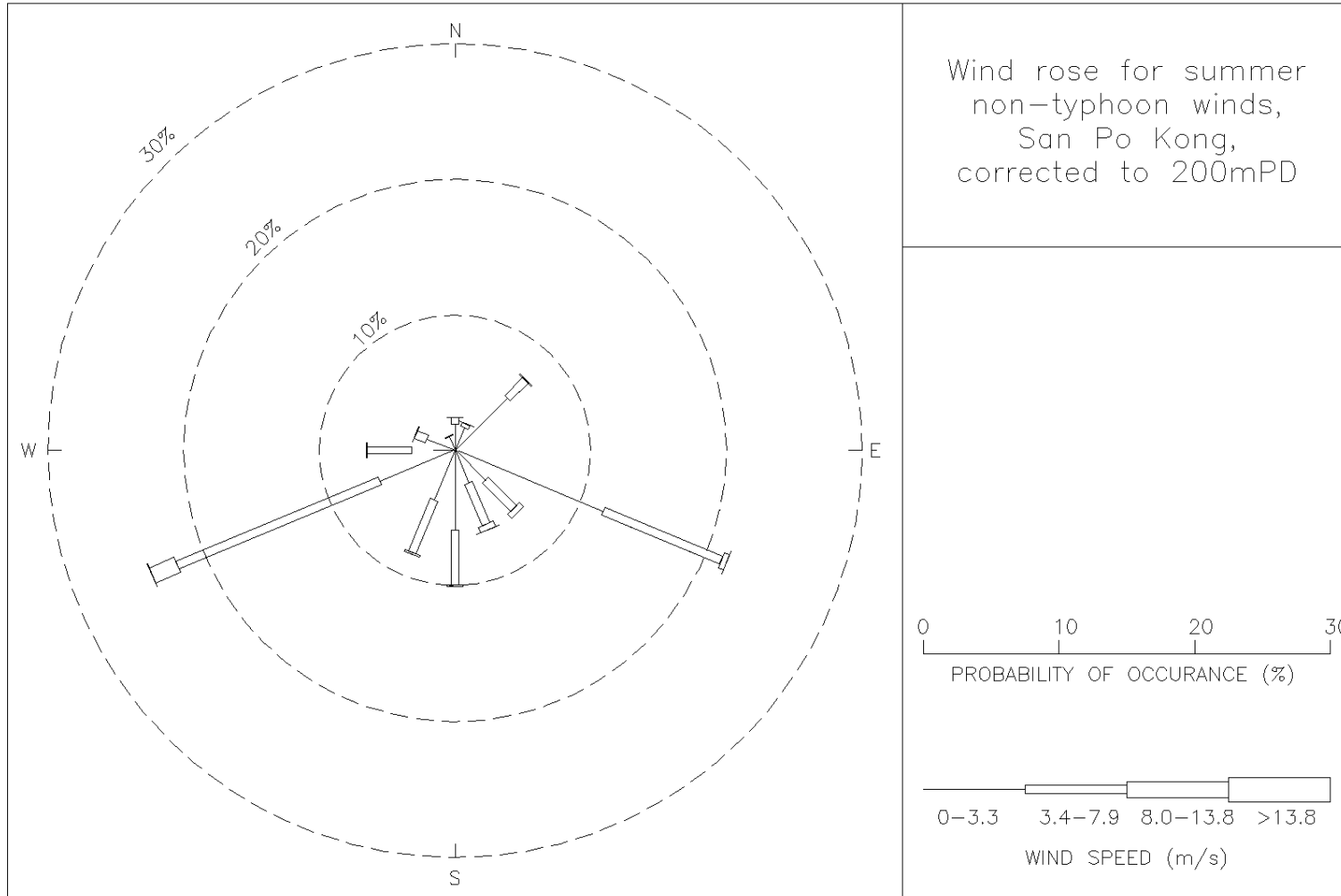


Figure 31: Wind rose for summer, non-typhoon winds for San Po Kong, corrected to 200 mPD

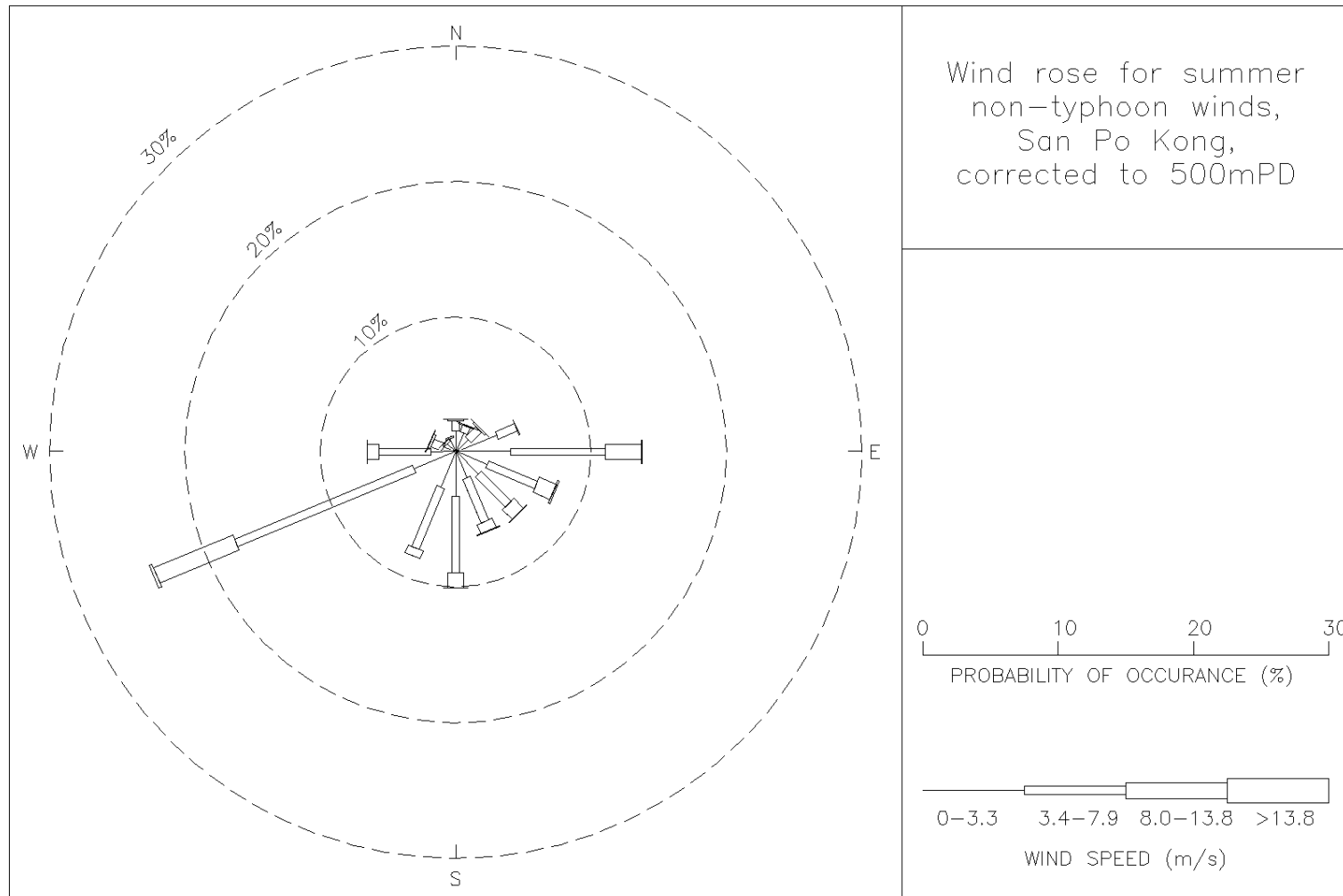


Figure 32: Wind rose for summer, non-typhoon winds for San Po Kong, corrected to 500 mPD

APPENDIX A
TABULATED RESULTS FOR SAN PO KONG

Table A1: Site wind characteristics of San Po Kong at 22.5°

Prototype scale elevation (mPD)	Normalised mean wind speed	Turbulence intensity (%)	Pitch angle (°)	Yaw angle (°)
25	0.41	26.1%	-6.1	-11.6
50	0.43	26.3%	-6.4	-10.6
75	0.44	27.0%	-6.5	-10.1
100	0.46	27.2%	-6.5	-9.1
150	0.49	26.4%	-7.1	-8.0
200	0.53	25.7%	-6.9	-7.0
300	0.61	23.4%	-5.9	-4.6
400	0.67	21.3%	-4.9	-2.6
500	0.71	19.8%	-3.8	-2.4

Table A2: Site wind characteristics of San Po Kong at 45°

Prototype scale elevation (mPD)	Normalised mean wind speed	Turbulence intensity (%)	Pitch angle (°)	Yaw angle (°)
25	0.38	22.3%	-4.3	-2.6
50	0.39	22.6%	-3.7	-2.6
75	0.43	22.3%	-4.1	-2.8
100	0.43	22.6%	-3.8	-2.0
150	0.48	21.3%	-3.8	-2.4
200	0.52	19.8%	-3.6	-2.4
300	0.60	15.9%	-3.2	-4.0
400	0.65	14.9%	-3.0	-4.9
500	0.70	13.8%	-2.9	-5.9

Table A3: Site wind characteristics of San Po Kong at 67.5°

Prototype scale elevation (mPD)	Normalised mean wind speed	Turbulence intensity (%)	Pitch angle (°)	Yaw angle (°)
25	0.28	28.4%	-4.1	21.3
50	0.30	30.1%	-4.8	21.8
75	0.31	29.6%	-4.7	22.1
100	0.31	29.2%	-5.1	21.4
150	0.32	30.6%	-5.4	19.7
200	0.32	30.2%	-6.2	17.3
300	0.31	30.9%	-5.5	14.3
400	0.34	32.7%	-6.1	12.2
500	0.36	33.7%	-5.5	10.5

Table A4: Site wind characteristics of San Po Kong at 90°

Prototype scale elevation (mPD)	Normalised mean wind speed	Turbulence intensity (%)	Pitch angle (°)	Yaw angle (°)
25	0.24	28.4%	-2.2	6.0
50	0.26	30.7%	-3.0	2.0
75	0.27	32.0%	-2.4	-1.6
100	0.31	32.7%	-2.5	-5.6
150	0.37	30.0%	-2.1	-11.0
200	0.43	26.6%	-0.5	-14.3
300	0.54	21.4%	0.1	-14.9
400	0.61	18.5%	0.4	-13.4
500	0.70	15.2%	-0.3	-11.0

Table A5: Site wind characteristics of San Po Kong at 112.5°

Prototype scale elevation (mPD)	Normalised mean wind speed	Turbulence intensity (%)	Pitch angle (°)	Yaw angle (°)
25	0.34	21.1%	-6.7	12.9
50	0.36	23.4%	-6.6	10.5
75	0.39	24.5%	-6.3	6.7
100	0.42	25.7%	-6.3	3.4
150	0.49	24.1%	-4.8	-0.8
200	0.57	21.1%	-3.6	-3.9
300	0.70	15.7%	-2.5	-6.4
400	0.78	12.8%	-2.1	-6.9
500	0.84	10.6%	-1.7	-7.1

Table A6: Site wind characteristics of San Po Kong at 135°

Prototype scale elevation (mPD)	Normalised mean wind speed	Turbulence intensity (%)	Pitch angle (°)	Yaw angle (°)
25	0.37	21.6%	-6.8	8.7
50	0.40	22.8%	-6.5	7.4
75	0.44	22.7%	-6.5	5.8
100	0.48	22.5%	-6.0	4.9
150	0.57	19.5%	-4.7	3.1
200	0.67	15.1%	-3.5	1.4
300	0.78	10.4%	-2.1	0.2
400	0.83	8.1%	-1.0	-0.3
500	0.86	6.7%	-0.3	-0.4

Table A7: Site wind characteristics of San Po Kong at 157.5°

Prototype scale elevation (mPD)	Normalised mean wind speed	Turbulence intensity (%)	Pitch angle (°)	Yaw angle (°)
25	0.34	27.9%	-4.4	10.2
50	0.41	28.0%	-5.5	6.7
75	0.46	26.4%	-5.4	3.7
100	0.52	24.1%	-5.0	2.7
150	0.65	18.6%	-4.2	2.0
200	0.74	14.5%	-3.4	2.2
300	0.81	11.7%	-2.5	2.1
400	0.85	10.7%	-2.3	2.5
500	0.86	10.6%	-1.8	2.3

Table A8: Site wind characteristics of San Po Kong at 180°

Prototype scale elevation (mPD)	Normalised mean wind speed	Turbulence intensity (%)	Pitch angle (°)	Yaw angle (°)
25	0.28	24.3%	-4.3	4.3
50	0.30	26.2%	-4.3	1.9
75	0.32	27.5%	-3.3	1.3
100	0.35	28.5%	-2.7	1.1
150	0.42	27.1%	-1.5	-0.6
200	0.53	22.4%	-0.6	-2.0
300	0.67	15.0%	0.8	-2.5
400	0.73	13.0%	1.2	-3.0
500	0.79	12.4%	1.4	-3.9

Table A9: Site wind characteristics of San Po Kong at 202.5°

Prototype scale elevation (mPD)	Normalised mean wind speed	Turbulence intensity (%)	Pitch angle (°)	Yaw angle (°)
25	0.38	19.4%	-5.0	0.0
50	0.41	20.1%	-4.3	-1.3
75	0.43	20.6%	-3.8	-2.1
100	0.45	21.0%	-3.6	-2.8
150	0.50	20.6%	-2.7	-4.9
200	0.55	19.6%	-2.0	-5.7
300	0.61	18.3%	-0.9	-6.4
400	0.64	17.6%	0.3	-7.6
500	0.69	16.4%	1.3	-8.4

Table A10: Site wind characteristics of San Po Kong at 225°

Prototype scale elevation (mPD)	Normalised mean wind speed	Turbulence intensity (%)	Pitch angle (°)	Yaw angle (°)
25	0.42	22.7%	-2.4	-3.0
50	0.46	22.7%	-2.3	-4.6
75	0.52	21.5%	-2.3	-6.3
100	0.57	20.2%	-1.9	-7.9
150	0.65	17.0%	-1.8	-10.8
200	0.71	14.8%	-1.7	-12.2
300	0.80	11.5%	-1.1	-13.4
400	0.87	8.9%	-0.9	-13.6
500	0.91	7.3%	-0.4	-13.4

Table A11: Site wind characteristics of San Po Kong at 247.5°

Prototype scale elevation (mPD)	Normalised mean wind speed	Turbulence intensity (%)	Pitch angle (°)	Yaw angle (°)
25	0.39	18.0%	-4.0	4.5
50	0.41	18.3%	-3.3	3.4
75	0.45	18.2%	-2.9	1.9
100	0.48	17.9%	-1.9	0.6
150	0.53	16.8%	-0.8	-0.3
200	0.56	16.2%	0.0	-0.6
300	0.63	15.2%	0.9	-1.1
400	0.72	13.0%	1.4	-2.2
500	0.81	9.7%	1.6	-2.9

Table A12: Site wind characteristics of San Po Kong at 270°

Prototype scale elevation (mPD)	Normalised mean wind speed	Turbulence intensity (%)	Pitch angle (°)	Yaw angle (°)
25	0.31	26.4%	-1.5	3.8
50	0.34	26.9%	-0.5	3.4
75	0.37	26.6%	-0.2	3.3
100	0.41	25.9%	-0.1	3.2
150	0.47	23.3%	0.5	2.4
200	0.54	20.1%	0.6	1.5
300	0.66	14.9%	0.7	1.0
400	0.75	11.5%	1.1	0.8
500	0.82	8.5%	1.2	1.0

Table A13: Site wind characteristics of San Po Kong at 292.5°

Prototype scale elevation (mPD)	Normalised mean wind speed	Turbulence intensity (%)	Pitch angle (°)	Yaw angle (°)
25	0.39	20.9%	-3.7	6.3
50	0.42	21.7%	-3.6	6.0
75	0.46	21.8%	-3.6	5.7
100	0.49	22.0%	-3.3	6.2
150	0.54	21.0%	-2.9	6.8
200	0.59	19.2%	-2.4	6.7
300	0.69	15.2%	-1.9	5.4
400	0.77	12.6%	-1.8	3.7
500	0.81	11.3%	-1.4	3.1

Table A14: Site wind characteristics of San Po Kong at 315°

Prototype scale elevation (mPD)	Normalised mean wind speed	Turbulence intensity (%)	Pitch angle (°)	Yaw angle (°)
25	0.39	22.5%	-2.9	26.7
50	0.42	24.0%	-3.3	25.3
75	0.43	24.6%	-3.8	24.3
100	0.44	25.0%	-3.9	23.1
150	0.45	26.6%	-4.2	19.3
200	0.47	27.7%	-4.8	16.0
300	0.51	28.8%	-5.1	9.0
400	0.58	27.4%	-4.9	2.8
500	0.65	25.1%	-4.2	-1.8

Table A15: Site wind characteristics of San Po Kong at 337.5°

Prototype scale elevation (mPD)	Normalised mean wind speed	Turbulence intensity (%)	Pitch angle (°)	Yaw angle (°)
25	0.44	26.6%	-5.2	-3.7
50	0.47	26.7%	-5.1	-4.6
75	0.48	26.7%	-5.2	-2.8
100	0.49	27.1%	-5.1	-2.6
150	0.53	27.1%	-5.3	-1.2
200	0.54	28.1%	-4.7	0.6
300	0.55	28.1%	-3.8	2.6
400	0.58	27.3%	-3.5	2.4
500	0.58	28.0%	-2.0	2.4

Table A16: Site wind characteristics of San Po Kong at 360°

Prototype scale elevation (mPD)	Normalised mean wind speed	Turbulence intensity (%)	Pitch angle (°)	Yaw angle (°)
25	0.37	25.6%	-4.4	12.5
50	0.40	25.9%	-4.8	11.3
75	0.43	26.3%	-5.2	10.4
100	0.45	26.9%	-5.6	9.4
150	0.51	25.5%	-5.6	7.2
200	0.57	23.6%	-5.3	4.4
300	0.70	17.6%	-5.0	1.0
400	0.80	12.7%	-4.4	-0.4
500	0.86	10.3%	-3.9	-0.9

Table A17: Percentage occurrence for annual, non-typhoon directional winds at 50 mPD

Wind Angle	Percentage occurrence for wind speed ranges:				Total
	$0 < u \leq 3.3$ m/s	$3.3 < u \leq 7.9$ m/s	$7.9 < u \leq 13.8$ m/s	$u > 13.8$ m/s	
0°	0.0%	0.0%	0.0%	0.0%	0.0%
22.5°	6.1%	2.1%	0.0%	0.0%	8.3%
45°	17.1%	6.8%	0.0%	0.0%	24.0%
67.5°	0.0%	0.0%	0.0%	0.0%	0.0%
90°	17.8%	5.6%	0.0%	0.0%	23.4%
112.5°	3.9%	1.0%	0.0%	0.0%	4.9%
135°	2.7%	0.5%	0.0%	0.0%	3.1%
157.5°	2.6%	0.4%	0.0%	0.0%	3.0%
180°	4.0%	0.2%	0.0%	0.0%	4.3%
202.5°	2.4%	0.7%	0.0%	0.0%	3.1%
225°	2.8%	2.1%	0.0%	0.0%	4.9%
247.5°	2.0%	1.2%	0.0%	0.0%	3.2%
270°	2.3%	0.2%	0.0%	0.0%	2.5%
292.5°	1.4%	0.2%	0.0%	0.0%	1.6%
315°	0.0%	0.0%	0.0%	0.0%	0.0%
337.5°	7.4%	6.2%	0.1%	0.0%	13.7%

Table A18: Percentage occurrence for annual, non-typhoon directional winds at 100 mPD

Wind Angle	Percentage occurrence for wind speed ranges:				Total
	$0 < u \leq 3.3$ m/s	$3.3 < u \leq 7.9$ m/s	$7.9 < u \leq 13.8$ m/s	$u > 13.8$ m/s	
0°	5.1%	6.8%	0.2%	0.0%	12.1%
22.5°	5.5%	2.7%	0.1%	0.0%	8.3%
45°	15.9%	8.1%	0.0%	0.0%	24.0%
67.5°	0.0%	0.0%	0.0%	0.0%	0.0%
90°	14.8%	8.6%	0.0%	0.0%	23.4%
112.5°	3.5%	1.4%	0.0%	0.0%	4.9%
135°	2.4%	0.7%	0.0%	0.0%	3.1%
157.5°	2.2%	0.8%	0.0%	0.0%	3.0%
180°	3.8%	0.4%	0.0%	0.0%	4.3%
202.5°	2.1%	1.0%	0.0%	0.0%	3.1%
225°	2.0%	2.8%	0.1%	0.0%	4.9%
247.5°	1.6%	1.6%	0.0%	0.0%	3.2%
270°	1.9%	0.6%	0.0%	0.0%	2.5%
292.5°	1.3%	0.3%	0.0%	0.0%	1.6%
315°	0.0%	0.0%	0.0%	0.0%	0.0%
337.5°	1.0%	0.5%	0.0%	0.0%	1.5%

Table A19: Percentage occurrence for annual, non-typhoon directional winds at 200 mPD

Wind Angle	Percentage occurrence for wind speed ranges:				Total
	$0 < u \leq 3.3$ m/s	$3.3 < u \leq 7.9$ m/s	$7.9 < u \leq 13.8$ m/s	$u > 13.8$ m/s	
0°	3.4%	7.6%	1.2%	0.0%	12.1%
22.5°	4.5%	3.6%	0.1%	0.0%	8.3%
45°	14.4%	9.6%	0.0%	0.0%	24.0%
67.5°	0.0%	0.0%	0.0%	0.0%	0.0%
90°	0.0%	0.0%	0.0%	0.0%	0.0%
112.5°	12.1%	15.5%	0.7%	0.0%	28.3%
135°	1.9%	1.1%	0.1%	0.0%	3.1%
157.5°	1.5%	1.3%	0.1%	0.0%	3.0%
180°	2.8%	1.5%	0.0%	0.0%	4.3%
202.5°	1.7%	1.4%	0.0%	0.0%	3.1%
225°	0.0%	0.0%	0.0%	0.0%	0.0%
247.5°	2.5%	5.1%	0.6%	0.0%	8.2%
270°	1.4%	1.0%	0.0%	0.0%	2.5%
292.5°	1.2%	0.3%	0.0%	0.0%	1.6%
315°	0.0%	0.0%	0.0%	0.0%	0.0%
337.5°	0.9%	0.6%	0.0%	0.0%	1.5%

Table A20: Percentage occurrence for annual, non-typhoon directional winds at 500 mPD

Wind Angle	Percentage occurrence for wind speed ranges:				Total
	$0 < u \leq 3.3$ m/s	$3.3 < u \leq 7.9$ m/s	$7.9 < u \leq 13.8$ m/s	$u > 13.8$ m/s	
0°	1.9%	5.6%	4.3%	0.4%	12.1%
22.5°	2.7%	5.0%	0.5%	0.0%	8.3%
45°	2.5%	5.8%	0.5%	0.0%	8.8%
67.5°	8.0%	7.1%	0.0%	0.0%	15.1%
90°	4.1%	11.5%	7.7%	0.2%	23.4%
112.5°	1.8%	2.2%	0.8%	0.1%	4.9%
135°	1.5%	1.3%	0.3%	0.0%	3.1%
157.5°	1.3%	1.5%	0.2%	0.0%	3.0%
180°	1.7%	2.2%	0.3%	0.0%	4.3%
202.5°	1.3%	1.6%	0.2%	0.0%	3.1%
225°	0.0%	0.0%	0.0%	0.0%	0.0%
247.5°	1.6%	4.7%	1.9%	0.1%	8.2%
270°	0.9%	1.3%	0.3%	0.0%	2.5%
292.5°	0.5%	0.3%	0.1%	0.0%	1.0%
315°	0.5%	0.1%	0.0%	0.0%	0.6%
337.5°	0.9%	0.6%	0.1%	0.0%	1.5%

Table A21: Percentage occurrence for summer, non-typhoon directional winds at 50 mPD

Wind Angle	Percentage occurrence for wind speed ranges:				Total
	$0 < u \leq 3.3$ m/s	$3.3 < u \leq 7.9$ m/s	$7.9 < u \leq 13.8$ m/s	$u > 13.8$ m/s	
0°	0.0%	0.0%	0.0%	0.0%	0.0%
22.5°	2.0%	0.2%	0.0%	0.0%	2.2%
45°	6.0%	1.4%	0.0%	0.0%	7.4%
67.5°	0.0%	0.0%	0.0%	0.0%	0.0%
90°	12.0%	1.8%	0.0%	0.0%	13.8%
112.5°	6.3%	1.6%	0.0%	0.0%	7.9%
135°	5.1%	1.4%	0.0%	0.0%	6.5%
157.5°	5.2%	1.1%	0.0%	0.0%	6.4%
180°	9.2%	0.8%	0.0%	0.0%	10.1%
202.5°	6.0%	2.3%	0.0%	0.0%	8.3%
225°	7.5%	6.9%	0.1%	0.0%	14.5%
247.5°	5.5%	4.2%	0.0%	0.0%	9.7%
270°	5.7%	0.8%	0.0%	0.0%	6.5%
292.5°	2.6%	0.5%	0.0%	0.0%	3.2%
315°	0.0%	0.0%	0.0%	0.0%	0.0%
337.5°	3.4%	0.3%	0.0%	0.0%	3.7%

Table A22: Percentage occurrence for summer, non-typhoon directional winds at 100 mPD

Wind Angle	Percentage occurrence for wind speed ranges:				Total
	$0 < u \leq 3.3$ m/s	$3.3 < u \leq 7.9$ m/s	$7.9 < u \leq 13.8$ m/s	$u > 13.8$ m/s	
0°	2.2%	0.3%	0.0%	0.0%	2.5%
22.5°	1.9%	0.2%	0.0%	0.0%	2.2%
45°	5.8%	1.6%	0.0%	0.0%	7.4%
67.5°	0.0%	0.0%	0.0%	0.0%	0.0%
90°	10.7%	3.1%	0.0%	0.0%	13.8%
112.5°	5.5%	2.4%	0.0%	0.0%	7.9%
135°	4.5%	2.0%	0.0%	0.0%	6.5%
157.5°	4.1%	2.2%	0.1%	0.0%	6.4%
180°	8.8%	1.3%	0.0%	0.0%	10.1%
202.5°	5.2%	3.1%	0.0%	0.0%	8.3%
225°	5.1%	9.0%	0.4%	0.0%	14.5%
247.5°	4.1%	5.5%	0.1%	0.0%	9.7%
270°	4.7%	1.8%	0.0%	0.0%	6.5%
292.5°	2.5%	0.6%	0.0%	0.0%	3.2%
315°	0.0%	0.0%	0.0%	0.0%	0.0%
337.5°	1.1%	0.1%	0.0%	0.0%	1.2%

Table A23: Percentage occurrence for summer, non-typhoon directional winds at 200 mPD

Wind Angle	Percentage occurrence for wind speed ranges:				Total
	$0 < u \leq 3.3$ m/s	$3.3 < u \leq 7.9$ m/s	$7.9 < u \leq 13.8$ m/s	$u > 13.8$ m/s	
0°	2.0%	0.5%	0.0%	0.0%	2.5%
22.5°	1.8%	0.3%	0.0%	0.0%	2.2%
45°	5.5%	1.9%	0.0%	0.0%	7.4%
67.5°	0.0%	0.0%	0.0%	0.0%	0.0%
90°	0.0%	0.0%	0.0%	0.0%	0.0%
112.5°	11.8%	9.4%	0.4%	0.0%	21.7%
135°	3.2%	2.9%	0.4%	0.0%	6.5%
157.5°	2.6%	3.3%	0.4%	0.0%	6.4%
180°	5.9%	4.0%	0.1%	0.0%	10.1%
202.5°	4.0%	4.2%	0.1%	0.0%	8.3%
225°	0.0%	0.0%	0.0%	0.0%	0.0%
247.5°	6.0%	16.2%	2.0%	0.0%	24.2%
270°	3.2%	3.2%	0.1%	0.0%	6.5%
292.5°	2.3%	0.9%	0.1%	0.0%	3.2%
315°	0.0%	0.0%	0.0%	0.0%	0.0%
337.5°	1.1%	0.1%	0.0%	0.0%	1.2%

Table A24: Percentage occurrence for summer, non-typhoon directional winds at 500 mPD

Wind Angle	Percentage occurrence for wind speed ranges:				Total
	$0 < u \leq 3.3$ m/s	$3.3 < u \leq 7.9$ m/s	$7.9 < u \leq 13.8$ m/s	$u > 13.8$ m/s	
0°	1.6%	0.8%	0.1%	0.0%	2.5%
22.5°	1.5%	0.6%	0.0%	0.0%	2.2%
45°	1.3%	1.1%	0.1%	0.0%	2.5%
67.5°	3.3%	1.5%	0.0%	0.0%	4.8%
90°	4.1%	7.0%	2.7%	0.1%	13.8%
112.5°	2.5%	3.9%	1.4%	0.1%	7.9%
135°	2.3%	3.2%	1.0%	0.0%	6.5%
157.5°	2.1%	3.5%	0.7%	0.0%	6.4%
180°	3.3%	5.6%	1.1%	0.0%	10.1%
202.5°	2.9%	4.9%	0.6%	0.0%	8.3%
225°	0.0%	0.0%	0.0%	0.0%	0.0%
247.5°	3.3%	14.2%	6.3%	0.3%	24.2%
270°	1.8%	3.9%	0.9%	0.0%	6.5%
292.5°	1.0%	0.8%	0.2%	0.0%	2.0%
315°	0.8%	0.2%	0.0%	0.0%	1.1%
337.5°	1.1%	0.1%	0.0%	0.0%	1.2%

APPENDIX B
AXIS SYSTEM OF THE COBRA PROBE

The following figures show the standard axis system of the Cobra Probe:

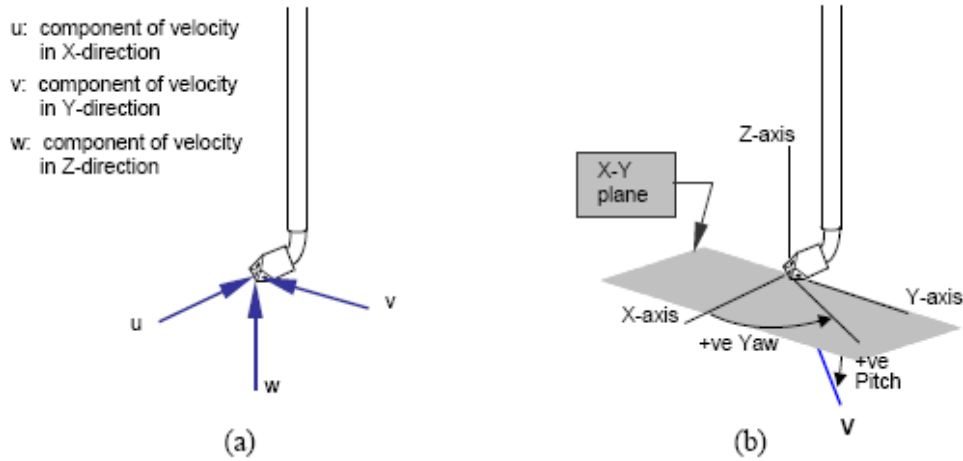


Figure B1: (a) Flow axis system with respect to the Cobra Probe head

(b) Positive flow pitch and yaw angles

Note: Yaw angle is technically 'azimuth' (rotation angle about the z-axis); Pitch angle is technically 'elevation' (the angle between the flow velocity vector V and the X-Y plane).